Finite element based simulation of diaphragm action on light weight composite plywood to sheet metal roof element.

Martin C. Kleven and Roald Norås

Norwegian University of Life Sciences
Department of Mathematical and technical sciences
Master Thesis 60 credits 2011

Preface

This study concludes a five year long study for two students at the University of Life Science. The extent of the study is 60 credits and based on a previous experiment done by Furulund and Thorrud in 2009 at the Norwegian University of Life Science in correspondence with Lett-Tak Systemer AS.

The motivation for this thesis was the wish to write a thesis involving wood science and mechanics. By choosing this assignment we have achieved both points, by studying diaphragm action in the light weight roof element using Finite element (FE) software.

This thesis aims to present some of the content from Furulund and Thorrud (2009) and Eli B. Rindal (2010). One of the focuses has been to make a thesis which may be published, therefore we have written the thesis in English. We have tried to be to the point, which means that the content not directly associated to the hypothesis is put in Appendixes. Therefore the study should be read together with the appendixes to get a complete understanding of the background for our choices and results. We expect the reader to have basic knowledge about FE-theory and general building science.

We would like to thank everyone who has made this study possible. Foremost among them thanks to Nils Ivar Bovim, our advisor who has given us inspiration and confidence along the way both professionally and personally. Thanks to EDR for introduction courses in software, helping us in the start of our process. Especially tanks to Jan Holdhus in EDR for support in SAP2000 along the way. Thanks to Dean Clark the lucky American who had the honor of "washing" Norwegian expressions out of the thesis. Thanks to Eli B. Rindal and Josef Tingnes who also contributed with proof reading.

Ås, 15. Mai 2011

Martin C. Kleven Roald Norås

Abstract

Two Finite Element (FE) models are built to simulate diaphragm action on light weight roof elements made of plywood, metal sheeting and solid wood rows. One model is simple and one is complex. The aim of this study is to verify the FE-models by full scale tests previously done. To compare the model and the tests both global and local deformations on the elements will be considered. The models will form a foundation for further development of FE- analysis based calculations for practical and scientific proposes on Lett-Tak AS.

The FE-models built has not fully been verified by the tests, but the model simulates and quantifies important effects observed in the test. Among these effects are increasing of shear capacity of the plywood diaphragm because large forces are transmitted to the edge-beams. And uplift forces because of eccentricity between the plywood panels and the support joint on the edge beam. It has been shown that the spring configuration used to model the fasteners in the gable support overestimates the stiffness and ultimate load of the fastener.

The FE-model developed in this study is a foundation for further research on stress and strain interactions between the material components and joints.

Contents

List of figures:

List of tables:

1. Introduction

1.1 Background.

The background of this paper is the need for more precise and efficient tools to analyze the behavior of light weight roof elements, due to diaphragm actions. Today, the analysis software is in constant development, offering a wide range of powerful options and tools. The growth in computer power makes these programs more accessible to the "main stream building industry". At the same time the industry is starting to demand more use of Building Information Modeling (BIM) software (Lett-Tak, 2011).

1.2 Previous work

The original light weight roof elements were developed in 1970-75 by the Norwegian Jens-Fredrik Larsen and the German professor Rolf Baehre (Furulund and Thorrud, 2009). The elements were made of sheeting metal and plywood. Today's element has been further developed and will be described in chapter 2 in this paper. Questions concerning statics on the original elements were treated by J.R. Larssen and report" R56:1975 is developing a basic bending theory for lightweight structural panels in single span under uniform load" (Larsen, 1975). In the spring 2009 Eirik Magnus Furulund and Kristian Thorrud wrote their thesis; Roof Diaphragms with Lightweight Structural Elements. Their aim was to "verify today's calculation methods and provide a foundation for future computer based analysis of the diaphragm actions" (Furulund and Thorrud, 2009). Tests of several types of fasteners and full scale test of three joined roof elements were done. Results from the tests provided us with necessary input data for our models. Eli B. Rindal continued Furulund and Thorrud's work, but with another approach. She wrote her thesis; 3D-modeling of Lightweight Roof Elements, autumn 2010. Her focus was opportunities within 3D modeling and BIM using TEKLA Structures. She also calculated the element's torsion stiffness and compared the calculated stiffness with a simplified FE-model (Rindal, 2010). After Rindal's thesis Larvik Lett-tak decided to research the possibilities of BIM and TEKLA Structures further. Rindal is currently working on finding a method of implementing TEKLA Structures in Lett-tak's production system (Lett-Tak, 2011). Even though no one has ever simulated the light weight roof element for Larvik Lett-tak with FEM software, it's natural to see the parallel towards modeling of monotonic and cyclic loading of diaphragm action on wood shear walls and

roofs. This has been handled thoroughly in a FEM setting by Erichsen et al (2007). and Judd (2005). This relation is discussed further in chapter 2.4.2.

1.3 The production today

The elements have been produced by Lett-Tak Systemer AS in Larvik since 1980. Larvik Lett-Tak produces more than 250 000 m^2 of roof elements each year (Lett-Tak, 2011). It is also produced in Austria and in the Czech Republic. Typical spans are 8-14 meters, and the maximum span is 18 meters. Today's analysis method is based on equilibrium and done in 2D. All of the calculations are done by hand. The principles of the calculations are shown in Skivekonstruksjoner med Lett-tak-elememter (Bovim 2009) and an example of their analysis is electronically attached (Sandved Arena). The work prints are done in AutoCAD, until Eli B. Rindal makes a good implementation of TEKLA Structures.

1.4 Objectives of the present study

Today's analysis of the diaphragm actions on lightweight roof elements are simple and good, but they lack accuracy, due to some important effects such as the F_v and F_h forces in the sheet metal, and the overall stress distribution between the components. The forces acting on the element can be decomposed into horizontal forces and vertical forces (F_v and F_h forces) between the metal sheeting and the edge beams (Figure1). Furulund and Thorrud found that the vertical forces reduce shear flow in the diaphragm perimeters. The horizontal forces cause the uplift forces because of eccentricity between the diaphragms and the edge beams (Furulund and Thorrud, 2009, Bovim, 2009). Figure 1 shows a standard light weight roof element. Furulund and Thorrud (2009) found that the shear capacity of the diaphragms was almost 50% higher than the expected value. Some of this potential may be used if the analysis model become more precise and take more of the 3-dimensional effects into account. Better information about interaction/stress distribution is of great value when analyzing more complex roof structures.

The goal of this thesis is to investigate how Lett-Tak AS can take advantage of modern software, to make their analysis more efficient and precise using FE-based software. This is done by using the experiment data from full scale tests to verify the FE-model. The verified FE-model will be a foundation for further investigation and practical implementation. The criterion when choosing a FE-software was that the program should have orthotropic shell elements, and supported non-linear analysis. Since Lett-Tak AS is considering starting to use

TEKLA Structures for modeling elements; our choice then became SAP2000, which is compatible with TEKLA Structures. In this study we have two models in which we compare the results from the experiments done by Furulund and Thorrud. One model is simple, with beam elements simulating the metal sheeting and shell elements to simulate the plywood. The other model has shell elements modeling the entire composite structure. The two models are named the beam model and the shell model. Two configurations of modeling the fasteners are also investigated. The interaction between SAP2000 and TEKLA Structures will not be investigated in this study.

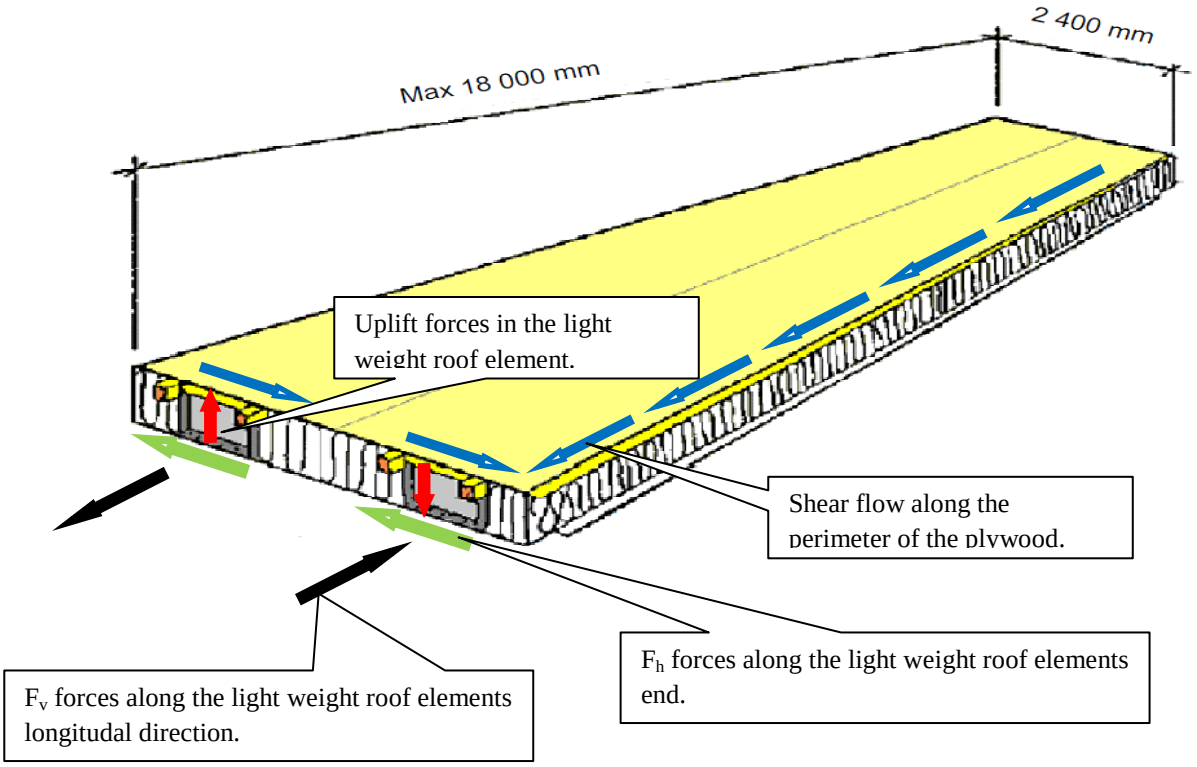

Figure 1: *One light weight roof element, maximum span is 18 m, the usual width is 2,4 m and the height (metal sheeting) span from 130 to 360 mm. The shear flow and corresponding F_h and F_v forces are shown. Picture is based on figures from Bovim 2009.*

2. Material and method

2.1 Light weight roof element

The light weight roof element (figure 1) studied in this paper consists of a sheet metal component (Figure 2c), shaped as a u channel. One to three sheet metal components are used in each panel, but two is common. Up to 360 *mm* high metal components are used for long spans, while in normal spans 210 *mm* height is used. The metal sheeting is cold rolled steel produced by Ruukki (Lett-Tak, 2011). At the top of the sheet metal there is a steel flange (Figure 2a) nailed and glued to the solid wood rows connecting the sheeting metal to the plywood panel. The solid wood rows (Figure 2a) are nailed and glued to the plywood panel (SINTEF Byggforsk, 1996). At the gable end of the roof elements, the sheeting metal is closed with a thicker support plate (Figure 2b), and a solid wood ribbon on top (figure 2c), to give the sheeting metal a higher stiffness at the support. In the case with edge beams made of glued laminated timber (GLT), screws are used to connect the end sheet metal to the edge beams. Screws are also used to connect the plywood to the edge beam and in the plywood panel butt joints at the perimeter between the roof elements (SINTEF Byggforsk, 2000). The butt joints are spliced with plywood which is glued on one side and screwed on the other to obtain the ductile behavior of the butt joint.

Figure 2a (left): *Upper steel flange and wood row.* ***Figure 2b (middle):*** *Support plate.* ***Figure 2c (right):*** *Support plate with wood ribbon mounted on metal sheeting. (Pictures are taken when the elements are mounted upside down in fabric.*

2.2 The full scale test

The full scale test was done with three roof elements each with a dimension of 7,2 x 2,4 meters. The edge beams consisted of GLT joined with hinges in all corners. A hydraulic cylinder was connected to the hinges on the diagonal B-D (Figure 3) to apply the load. Five tests were done with both 210-elements and 310-elements. For the 310-element, tests 1 and 2 were done with a maximum applied load of approximately 35*kN*, and with 200 *mm* screw spacing. In test 3 and 4 the spacing was decreased to 100 *mm* and the maximum applied load for test 3 was approximately 67 *kN*. In test 4 they tried to reach the ultimate load of the model but complete failure was not achieved, the loading stopped at 143 *kN*. Because failure did not occur, the light weight roof elements were unloaded and spacing was increased to 200 *mm* again. The fifth test reached failure at 98 *kN*. For further details about the experiment setup see Furulund and Thorrud's thesis (2009).

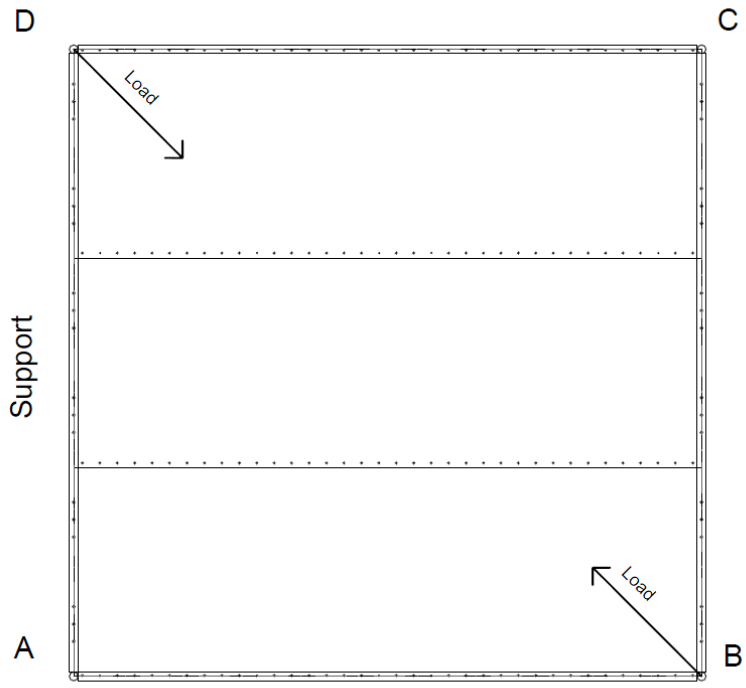

Figure 3: *Scheme for the full scale test, showing the plywood with its fasteners and the glue laminated timber edge beams with support. Based on pictures from Furulund and Thorrud(2009).*

2.3 Finite element model

Considering the scale of this thesis the FE-model is developed for the 310 *mm* elements only. The 310 *mm* elements in the full scale tests were tested with two different screw spacing's, 100 *mm* and 200 *mm*. Two sets of link elements have been made to simulate the fasteners in both cases. The modeling process is described in detail in appendix A.

In the beam model frame elements represent the sheet metal component together with the wood rows. The shell model uses shell elements to represent the sheet metal component and the wood rows. Our intention was to have one model with as simple a configuration as possible, but with sufficient accuracy for practical purposes. The shell model is supposed to be more accurate than the beam model, due to the complexity of the shell element and more detailed solutions with respect to fasteners. The shell model would also allow us to analyze stresses and buckling behavior in the metal sheeting in addition to the plywood.

In both models the edge beams are modeled with the general beam-column formulation in SAP2000. The insertion point is chosen to the center of mass, and a "dummy "element connects the longitudinal element with the gable element. The dummy element is a beam element with zero weight and it is stiff, but not to an unrealistic degree, to prevent numeric errors (Wilson, 2004). A normal steel section's stiffness's has been multiplied by 100. Dummies are used in both models. The dummies are described further in chapter 2.4.1

In the experiment the GLT beam is bolted to the concrete along A-D. The bolts started about 300 *mm* from each corner and 600 *mm* further along the beam (A and D). The GLT frame is held up from the floor with a trolley at B and C (Figure 3). To model the experiment we have put restraints along A-D, one at B and one at C. On A-D the GLT beam is restrained in the z-direction along all of its length. It is pinned down in three joints 300 *mm* from the corners A and D and 600 *mm* along the GLT beam. We have used a roller in B and C to prevent uplift in C and negative z-deformations in B. Furulund and Thorrud used weights at C to prevent uplift.

The hinges in the corners are modeled by releasing the dummy which connects the end-beams together. The dummy is released in the torsional degree of freedom. The GLT beam is also restrained against rotation about its own axis. $R_2(y)$ for A-D and B-C and $R_1(x)$ for A-B and C-D. This is done due to the rotational stiffness provided by the hinges in the corners.

In addition to modeling the full scale test a section from both models have been taken, to compare the torsion stiffness with the torsion stiffness found by Rindal (2010). The section is modified to be as similar to Rindal's setup as possible. The calculations are shown in appendix D.

2.4 Software (SAP2000)

SAP2000 is a stand-alone FE-based analysis and design program developed by Computers and Structures Inc. (CSI). It is made primarily for design and analysis of civil structures. SAP2000 is object-based, meaning that a beam with multiple members framing into it is created as a single object. The engine used for analysis is SAPfire (CSI, 2011). In the following chapters the elements used in the FE-model is described.

2.4.1 The Beam Element

From a geometric point of view, a beam is a structural component in which the longitudinal direction is considerably larger than the two other directions. From basic FE-theory a beam element is a line between two nodes (I and J), each with 6 degrees of freedom. SAP2000 uses the same notation (CSI, 2011a). A beam can be subject to bending and shear about the two orthogonal axis's, torsion about its own axis and axial deformations (Bell, 1994, CSI, 2011a). The beam element has its own local coordinate system like the other elements in SAP2000. The default insertion point is in the neutral axis of the beam. It is possible to change the insertion point to respond to geometric properties(CSI, 2011a). A change in insertion point causes the beam element to have a constraint connecting the line between the insertion points to the neutral axis of the frame element (CSI, 2011a). In our model both the custom beam section of the roof element (described in chapter 2.4.1) and the GLT are modeled as beam elements. Due to the distance between the beam's neutral axis and the other elements in the model the insertion point had to be moved or dummies had to connect the end-beams to the other parts of the model. In this study dummies have been used, making the model easier to work with and read.

There are several types of beams in the FE-model, the GLT, the dummies, and the composite section. The section designer option was used to model the composite section and the GLT section, because there were no predefined sections which matched our cross-sections.

The composite cross section represents the wood rows along the elements longitudinal direction, and the sheet metal component as shown in (Figure 4). To make the beam element

as close to the real cross section as possible a non-prismatic beam element, combining the two cross sections was made. The section to the right in figure 4b is the end section; the thicker support-plate with the wooden ribbon is described in part 2.1. The left side of figure 4b represents the cross section of the non-prismatic beam element between the supported ends of the beam element.

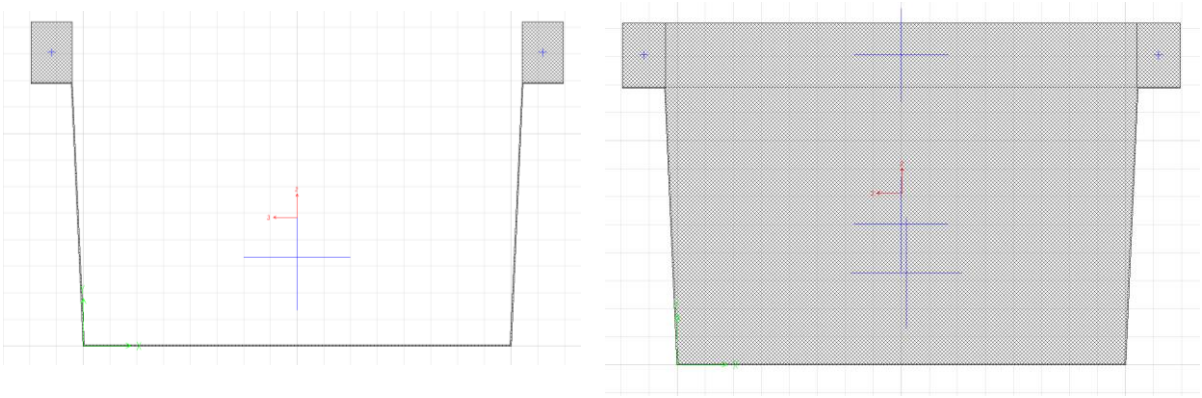

***Figure 4a Left**: Cross section made using the section designer option. The light weight roof element modeled as a beam element.* ***Figure 4b Right:** The end-section of the beam element modeling the light weight roof element.*

In the beam model the dummies are used to connect the neutral axis of the non-prismatic beam element to the plywood and the support beams (Figure 5). In addition the dummies connect the GLT beam along the perimeters of the plywood. (A-B and C-D). The dummies make the non-prismatic beam rotate with the plywood panel and the supporting beams. This corresponds with the FE-model made by Eli B. Rindal (2010).
In the shell model the dummies are used to connect the shell elements in the gable to the support beam (Figure 6) and dummies along the A-B and C-D connects the GLT beam to the plywood panel.

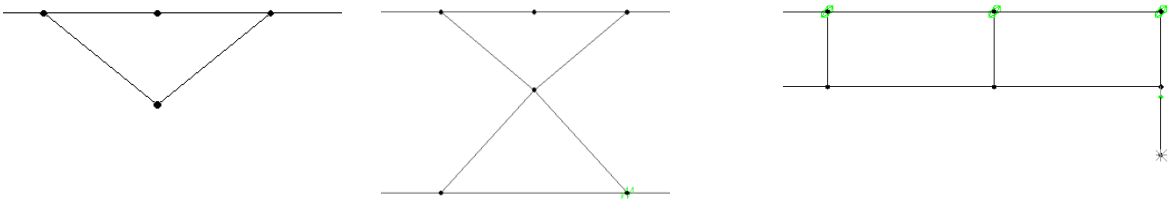

Figure 5: *Dummies in the beam model connecting the neutral axis of the non-prismatic frame element to the plywood panel (left), the neutral axis to the support and plywood panel (middle) and the GLT-beam to the plywood panel.*

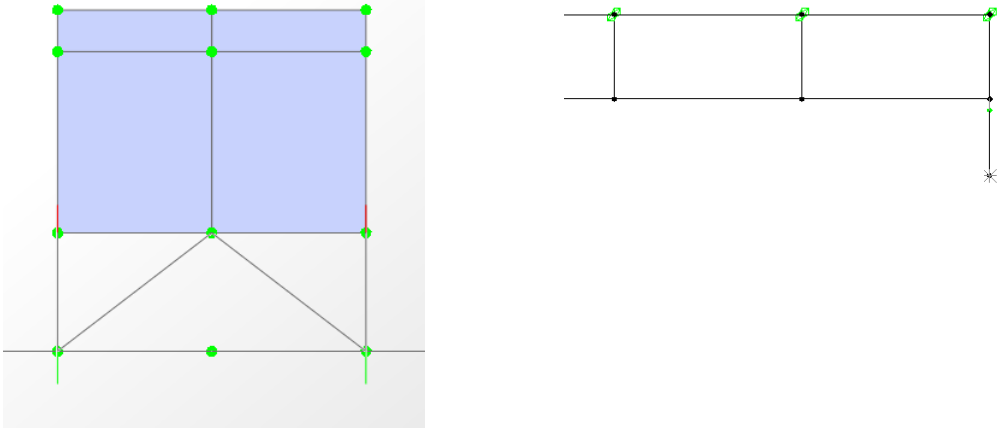

Figure 6: *Dummies used in the shell model to connect the sheeting metal elements to the GLT beam in the gable of the element (left) and the GLT beam (A-B and C-D) to the plywood panel (right)*

2.4.2 Shell Element

From basic FEM-theory a quadratic plate/shell is an element with 8 nodes, 4 nodes in each plane (Felippa, 2004). In SAP2000 the elements are made using 4 primary nodes in the plane of insertion and 4 secondary nodes. By definition the shell element can be subject to forces perpendicular to its plane and in its own plane (Wilson, 2004, Bell, 1994, Huebner et al., 2001, Schueller, 2008). This is the case in SAP2000 (Wilson, 2004, Schueller, 2008). SAP2000 has elements which can be subject to only transverse forces and only perpendicular forces, respectively membrane elements and plate elements (CSI, 2011a, Wilson, 2004). The shell element is a combination of these two elements (Wilson, 2004, CSI, 2011a, Schueller, 2008). There is an option to choose the ratio between plate and membrane action of the shell element. Both values are set to the thickness of the shell elements used in the research done by Furulund and Thorrud (2009). For membrane behavior an isoparametric formulation is used, including translation in plane stiffness and a drilling rotational stiffness component (CSI, 2011a). The drilling rotational stiffness means the stiffness about its normal plane (CSI, 2011a).

In both models the plywood panels are simulated with shell elements. The shell elements have the same thickness as the plywood panel in the full scale test and thin- shell properties. The thin-shell option (Kirchhoff) means that for plate-bending the shell will neglect transverse shear deformation. For thick shells (Mindlin/Reissner) the transverse shear deformation is taken into account (CSI, 2011a).

In the shell model all of the light weight roof elements are modeled using shell elements. The steel sheeting sections and plywood panel have thin-shell properties and the wooden rows have thick-shell properties due to its thickness. The plywood panel have same properties in both models.

2.4.3 Link elements

The behavior of sheeted wood shear panels is essentially dependent on the characteristics of the wood sheeting to frame fasteners. (Girhammar et al 2004., Judd, 2005,Vessby et al., 2010) Different methods have previously been used to model fasteners; single spring and orthogonal uncoupled springs (Vessby et al., 2010), different types of orthogonal coupled springs (Vessby et al., 2010). Coupled behavior means that the spring stiffness and spring forces are functions of the displacement in x- and y-direction (Judd, 2005).

An uncoupled single spring is the simplest configuration, a problem with it is that zero stiffness is gained for forces perpendicular to the spring direction. Such a spring could lead to numerically difficulties if the trajectory of the spring is considerably changed (Vessby et al., 2010). According to Judd (2005) the single spring is particular unstable when the ultimate load is reached. Another problem with the single spring is the opportunity to take into account the orthotropic behavior of wood (Vessby, 2010) however this is not critical for fastener dimensions less than 6 mm (Bovim, 2011).

The drawback of using orthogonal uncoupled springs is that it overestimates the capacity of the fastener, if the displacement follows both directions (Judd, 2005, Vessby et al., 2010). Judd (2005) proposed to use a coupled oriented spring pair with predefined (often initial) trajectory to solve this problem.

Special elements for simulating fasteners are not common in standard FE-software. Thereby the available spring elements in SAP2000 are used in this study. Two configurations of simulating fastener have been studied. Primary an uncoupled three dimensional spring model, similar to the uncoupled orthogonal spring used by Judd (2005) and Vessby et al. (2010). Secondary we have experimented with a single spring. The coupled and uncoupled springs are presented schematically in figure 7.

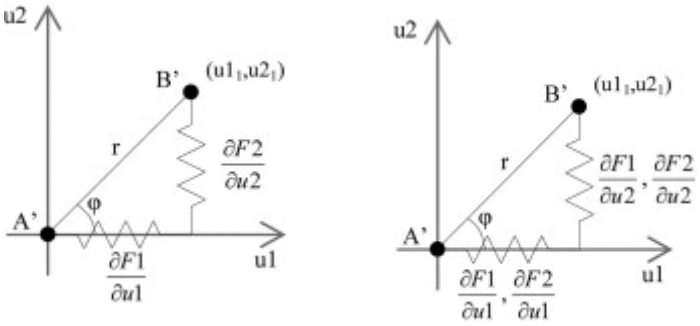

Figure 7: *Orthogonal uncoupled springs and coupled springs. The three-dimensional uncoupled spring are in principle equal to the uncoupled springs. Figure from Vessby et al. (2010).*

Due to the nonlinear behavior of the load-slip curves found by Furulund and Thorrud, the multi-linear elastic link element in SAP2000 is used to model the fasteners. The multi-linear elastic link element has 6 degrees off freedom (DOF) and can have independent load-slip curves specified, meaning that all degrees of freedom have independent deformations (CSI, 2010). The stiffness of the fasteners is based on the experiment done by Furulund and Thorrud in 2009. They tested the load carrying shear capacity for single shear connection plywood-to-plywood (Figure 8c), in 20 series of 4 single fasteners. The screw type is IWF-T dimension; 5x45 *mm*, quality; 8.8, producer; SFS Intec AS (Furulund and Thorrud, 2009). The same screw was used for plywood-to-edge framing fasteners in the test, and the same test data as above is used in this thesis for the plywood to edge beam fasteners. The shear (Figure 8b) and withdrawal (Figure 8a) load carrying capacity for the fasteners between the metal sheeting and the edge beams were tested, in 20 series of respectively 2 and 1 fasteners. The screw type is special produced for Lett-Tak, dimension; 10x100 *mm*, quality; 8.8. Load-slip data from fastener tests and a Foschi based simulation of fastener behavior are shown in figure 8. The reason for deviation between analysis curve and Foschi curve (Figure 8) is that the analysis curve used in analysis models is scaled to simulate a certain number of fasteners.

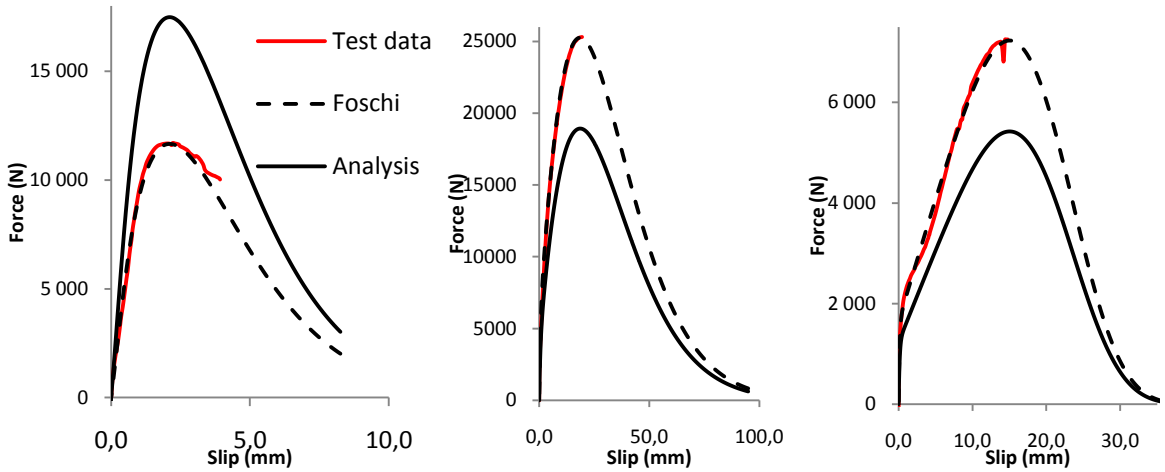

Figure 8: *Load slip curves.* ***8a (left):*** *Withdrawal of gable fasteners.* ***8b (middle):*** *Shear of gable fasteners* ***8c (right):*** *Shear of fasteners in plywood panel butt joint.*

For the withdrawal capacity of the fasteners in the perimeter joints, we had to do hand calculations due to lack of empirical values. The hand calculations are a conservative simplification. The calculated capacity is in accordance with Eurocode 5 (CEN, 2004) and shown in appendix C.

The gable fasteners are loaded by both tension and compression forces due to the rotation of the elements (Furulund and Thorrud, 2009). The fasteners with tension forces are modeled with a link element using the load-slip curves found in Furulund and Thorrud for both withdrawal and shear. The fasteners with compression forces are modeled by the same load-slip curve for shear, but the z-direction is fixed. This assumption is taken because the GLT beam and the support plate is relative stiff with respect to buckling of the support plate and compression of the wood in the GLT beam. Thereby it keeps the element from moving in negative z-direction (Figure 9) a load-slip curve simulating this behavior would be complicated to achieve.

Figure 9: *Buckling in the sheeting metal and compression of GLT. The picture is taken from Furulund and Thorrud's thesis.*

The mean values from the fastener test was plotted in excel and modeled with a 5-parameter Foschi-based equation, which simulates the ductile behavior of the fastener.

$$P = (P_0 + K_1 u)\,(1 - e^{-\frac{K_0 u}{P_0}})\,e^{-\frac{u^{\alpha}}{\beta}}$$

Figure 10: *5- parameter Foschi-based equation.*

The Foschi based equation in figure 10 and has been proposed by Girhammer et al. The equation contains the three basic parameters used by Foschi: K0, K1 and P0, to simulate respectively, slope at initial stiffness, slope at the first asymptote, and interception point on the first asymptote (Figure 11). Two additional parameters, α and β is used to simulate the point of failure and the softening behavior of the fastener. See appendix C for details about the fasteners.

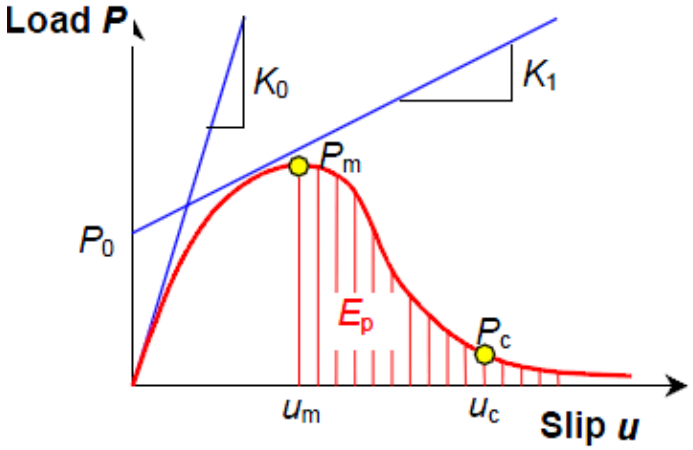

Figure 11: *Load slip curve. From (Girhammar et al.)*

The fastener spacing used in Thorrud and Furulund was 200 *mm* and 100 *mm*. In this study both spacing's are modeled in SAP2000 for the 310 *mm* element. The original link element distance was 600 *mm* based on practical considerations due to the roof element size. This implicates lumping respectively 3 and 6 fasteners together. Three models with three different link element distances respectively 300 *mm*, 600 *mm* and 1200 *mm* have been investigated to view how the link element distance influences the results.

2.4.4 Analysis method

To model the nonlinear effect of the model, the p-delta effects and the non-linear behavior of the fasteners, a nonlinear static analysis is used. SAP2000 uses the fast nonlinear analysis (FNA) method to analyze nonlinear behavior. The FNA is faster and more accurate compared to the traditional analysis methods for nonlinear analysis (Wilson, 2004). The traditional methods for analysis are using exact eigenvectors to solve the equations. The FNA uses load dependent Ritz vectors for more accurate results and less computational time (Wilson, 2004). More details about the analysis method are shown in appendix G.

2.4.5 Material inputs to FE-models.

The materials used in this thesis have been chosen based on the experiment done by Thorrud and Furulund. They found some of the values by testing materials used in the full scale test; density of the GLT and plywood. This and other material input data is presented in Table ***2***. SAP2000 has no predefined properties for timber materials thereby new materials were defined for all of the wood based materials: plywood, wood and GLT. Orthotropic behavior is chosen in SAP2000 for of GLT, solid wood and plywood. For simplification, the input data is manipulated to simulate transverse isotropic behavior for solid wood and GLT. See appendix B for further information about the material input used in the model.

Table 2: *Material input data for SAP2000*

Structural-component	**Thickness**	**Material data**
Plywood sheeting	15 mm	Directional symmetry type = Orthotropic Weight per Unit Volume = 4,511e-6N/mm³ (7) Modulus of elasticity E_1= 7 200 E_2= 5 133 N, E_3 = 200 N/mm² (2)(6) Poisson's Ratio, U_1 = 0,1, U_2 = 0,1, U_3 = 0,1 (6) Shear Modulus, G_{12} = G_{13} = 350 N/mm² G_{23} = 35 N/mm² (2)
Metal sheeting Support plate	1,2 mm 2 mm	Weight per Unit Volume = 7,85-05N/mm³ (1) Modulus of elasticity, E = 210 000N/mm² (1) Poisson's Ratio, U = 0,3 (4) Shear Modulus G = 81000 (1) Minimum Yield stress, F_y = 355 N/mm²(4) Minimum Tensile Stress, F_u = 400 N/mm²(4)
Wood - C24		Directional symmetry type = Orthotropic Weight per Unit Volume = 4,119e-6 N/mm³ (3) Modulus of elasticity E_1=11 000, E_2 = E_3 = 370 (5)(6) Poisson's Ratio, U_1 = U_2 = U_3 = 0,1 (6) Shear Modulus, G_{12} = G_{13} = G_{23} = 690 N/mm² (6)
GLT - Glued Laminated Timber		Directional symmetry type = Orthotropic Weight per Unit volume = 4,511-6N/mm³ (7) Modulus of elasticity: E_1= 13700, E_2 = E_3 = 420 (5)(6) Poisson's Ratio, U_1 = U_2 = U_3 = 0,1 (6) Shear Modulus, G_{12} = G_{13} = G_{23} = 780 N/mm² (6)
Dummy	15 mm	Same as Metal sheeting/support plate. Section modifiers: weight = 0.

(1) Furulund and Thorrud, 2009
(2) Sintef Byggforsk, Technical approval, Wisa-Spruce plywood
(3) EN338 2009
(4) Default material settings SAP2000
(5) Excel spreadsheet from Lett-Tak AS
(6) Appendix C
(7) Density tests by Furulund and Thorrud.

2.5 Uplift forces

Furulund and Thorrud found that there is a considerable amount of uplift forces which reaches its peak at joint C. The results correspond with the calculations done by Nils I. Bovim (2009),

which show that the uplift is due to the horizontal forces (F_h) acting on the elements. In the experiment, Furulund and Thorrud put weights on the elements in corner C to counteract the uplift forces. The weight is not numerically documented, but it has been estimated to be about 600 kg by looking at pictures from Furulund and Thorrud. When modeling the uplift forces a 6 *kN* force in C was used.

2.7 Shell stress distribution

The F_h and F_v forces described in Bovim (2009), and Furulund and Thorrud (2009) are the decomposition of the forces acting on the light weight roof element. The forces are taken from the frame, through the fasteners and sheeting metal component to the plywood panel. They make a shear flow along the edges of the plywood panels. Figure 12 shows the force distribution, these forces cause the shear stress (σ_{xy}) and figure 1 shows the F_v and F_h forces. Furulund and Thorrud found that the shear forces give the elements a considerably larger ultimate stress capacity than expected. The vertical shear forces give a strain in the gable fasteners and some of the force is taken as tension perpendicular to the grain of the GLT beam. Having an analysis in three dimensions makes it possible to view the effects of the F_h and F_v forces and the corresponding stresses in detail. In SAP2000 the stress distribution are shown as average values, and varies linearly through the element. For thick-shells the stress is computed directly from the shear deformations. In the thin-shells element the stress is calculated based on the moment, because the transverse shear forces are assumed to be zero.

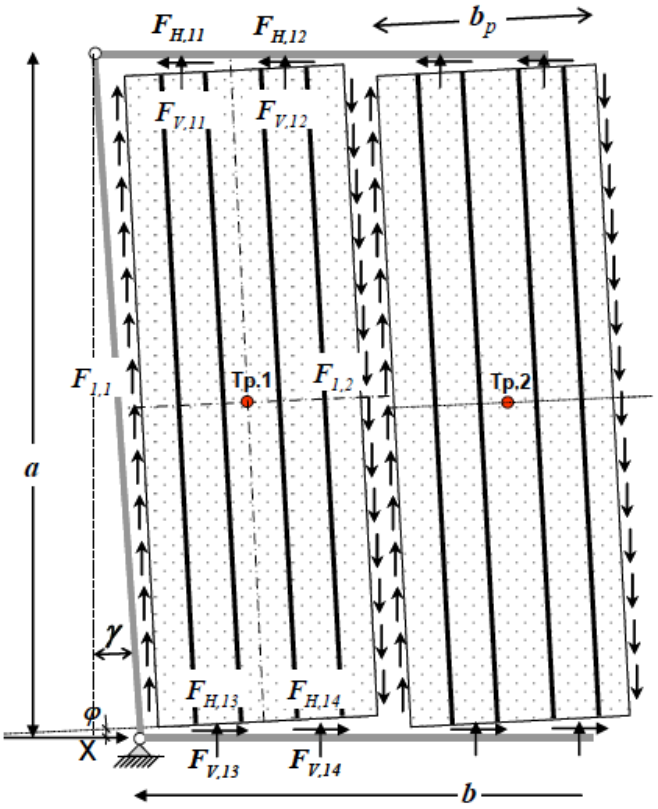

Figure 12: *Shell force distribution, shear flow along the plywood perimeter. From Bovim 2009.*

2.6 Important issues

The mesh is based on the original link element distances; 600 *mm*, the same method has been used in Wall Panel by Erichsen et al (2007). Free meshing is done by halving the size of the elements until sufficient convergence is reached. In this study the mesh size has been halved and doubled to view the effect of mesh size and a strict quadrilateral mesh is used. The angle in all corners is 90 degrees and all nodes in the shell element are coplanar. Erichsen et al, (2007) found no difference in the results for their model for meshes bigger or smaller than 300 *mm* * 300 *mm*.

The SAP2000 reference manual recommends aspect ratios less than four, and absolutely not bigger than ten. Thin plate theory (Kirchhoff) is less affected by the aspect ratio than thick plate theory (Reisner/Mindlin) (CSI, 2011a). A thick shell should have an aspect ratio between 10 and 20, if not thin shell properties should be chosen (CSI, 2011b). The highest aspect ratio is 12,5, in the wood rows. All the other elements have an aspect ratio smaller than four. The aspect ratio is directly dependent on the meshing hence the mesh size is expected to affect the results.

3. Results and discussion

The results from the analysis are compared with the tests done by Furulund and Thorrud (2009) and the simplified FE-model from Eli B. Rindal (2010). The placement of the transducers is shown in figure 13, with the corresponding notation. Delta X_1 is the relative displacement in the perimeter joints between the GLT beam and the plywood. Delta X_2 is the relative displacement on the plywood panel butt joint between element two and three. The transducers in the tests were placed on the side of the GLT in the middle of the beam height. In the analysis model the deformation in Y-direction is measured in B and C (figure 13) in the neutral axis of the GLT beam which corresponds to the placement of the transducers in the tests. The global Y-deformation shown in the results are the average of Y_1 and Y_2.In addition we have measured the uplift forces in C (z_2).The results are displayed graphically, the analysis models with the same link element distance are shown in the same graph. We have chosen to show the results from the comparison of the average global deformation in y-direction, slip in the joints on the plywood perimeters (delta X), link element forces, torsion stiffness, shell stress distribution, buckling behavior, uplift deformations, mesh size and link element distance. The data corresponding to the graphs and the tables in the results chapter is attached electronically.

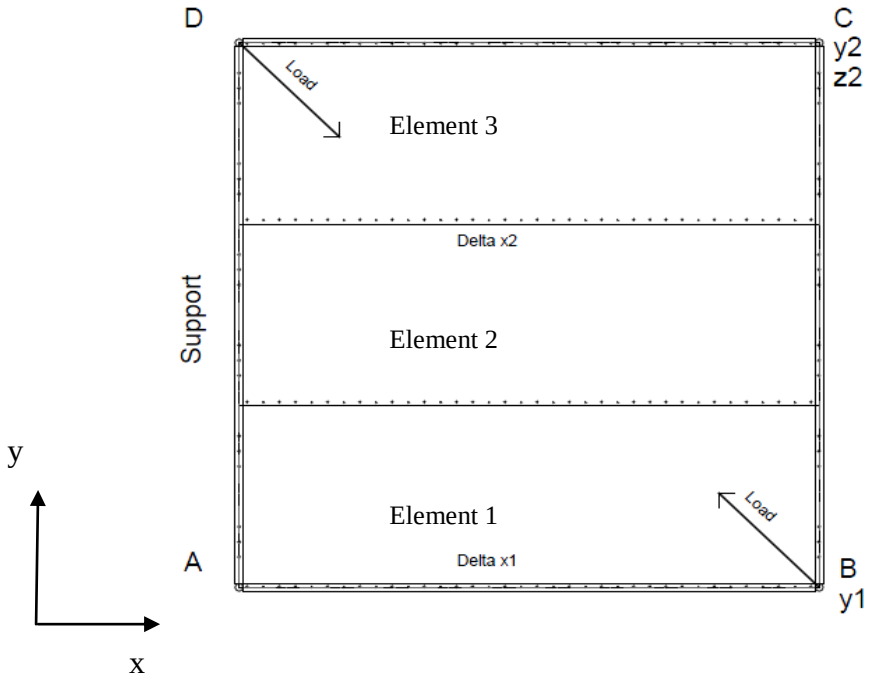

Figure 13: *Placement of the transducers in the full scale test (Furulund and Thorrud, 2009). Delta x_2 is the relative displacement on the plywood perimeter between element two and three and delta x_1 is the relative displacement between the GLT beam and the plywood in element 1. The deformations in y-direction are measured in B and C in the neutral axis of the GLT beam. In addition we have measured the uplift forces in C (z_2)*

3.1 General

The models are loaded by forces from 0 to 140 *kN*, with an interval of 10 *kN*. In addition we added 35 *kN* and 95 *kN*. The model changes from the linear elastic range to the plastic range at approximately 35 kN. At 95 kN the failure was observed in test 5.

Tests 1 and 2 have 200 *mm* fastener spacing, and tests 3 and 4 have 100 *mm* fastener spacing. Figure 14a and 14b show the deformations in y-direction for the models with 100 *mm* fasteners, while 15a and 15b corresponds to the 200 *mm* spacing.

Figures 17-20 show the relative deformation in the fasteners (delta X). The linear elastic range for the relative deformation of the fasteners is shown in the electronic attachments (results.xlsx).

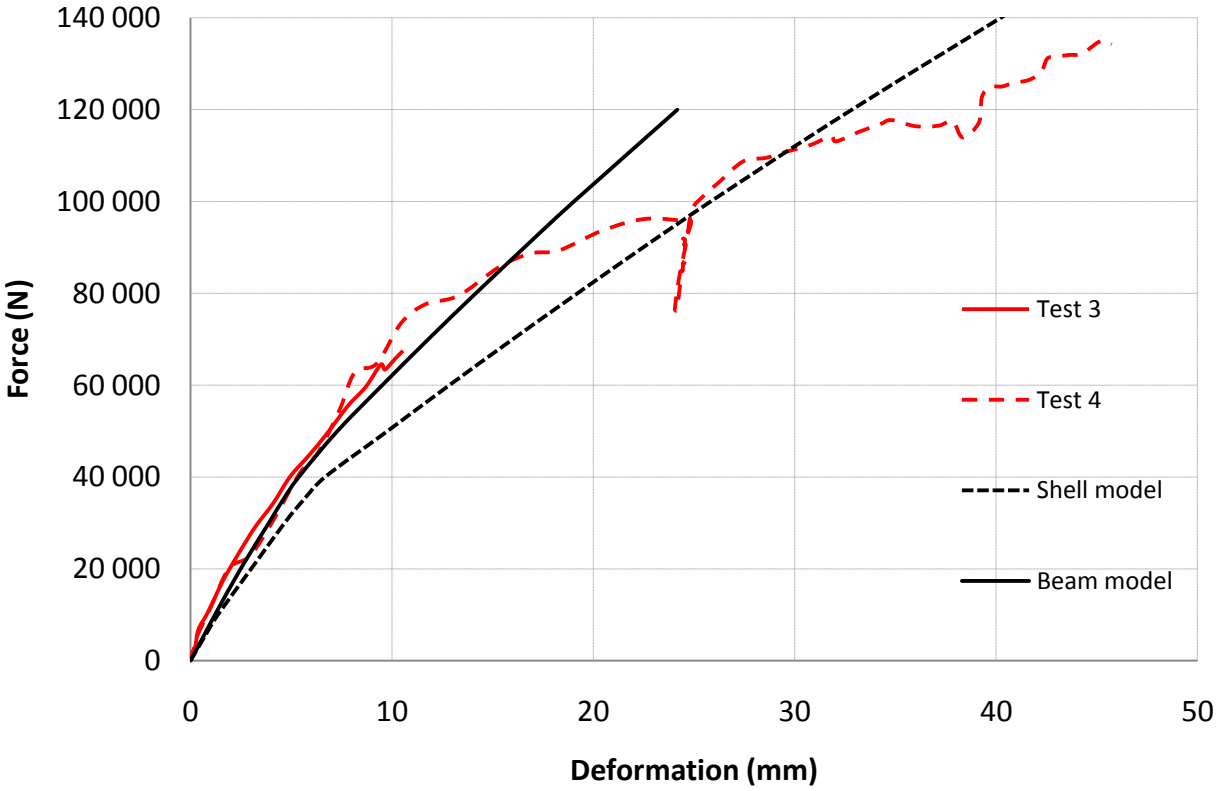

Figure 14a: *Load-slip curve for models and full scale tests with a fastener spacing of 100 mm. The deformations are an average of the deformation in Y_1 and Y_2. The test results are from Furulund and Thorrud 2009.*

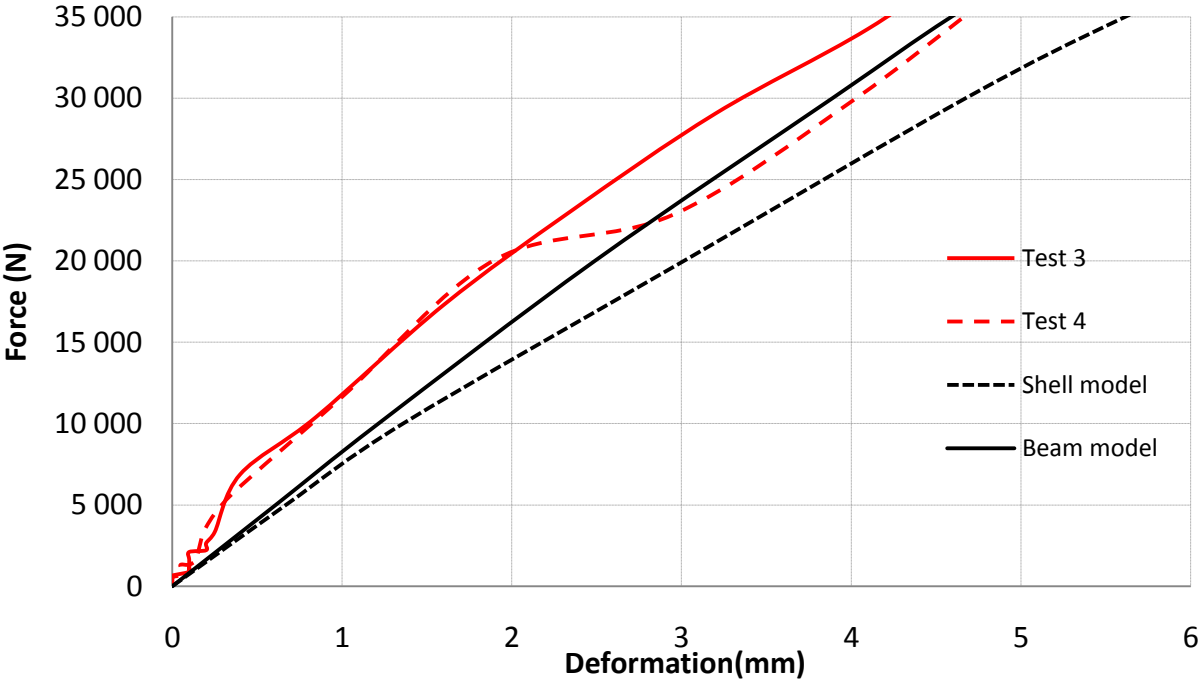

Figure 14b: *Average of Y_1 and Y_2 linear-elastic range. The test results are from Furulund and Thorrud 2009*

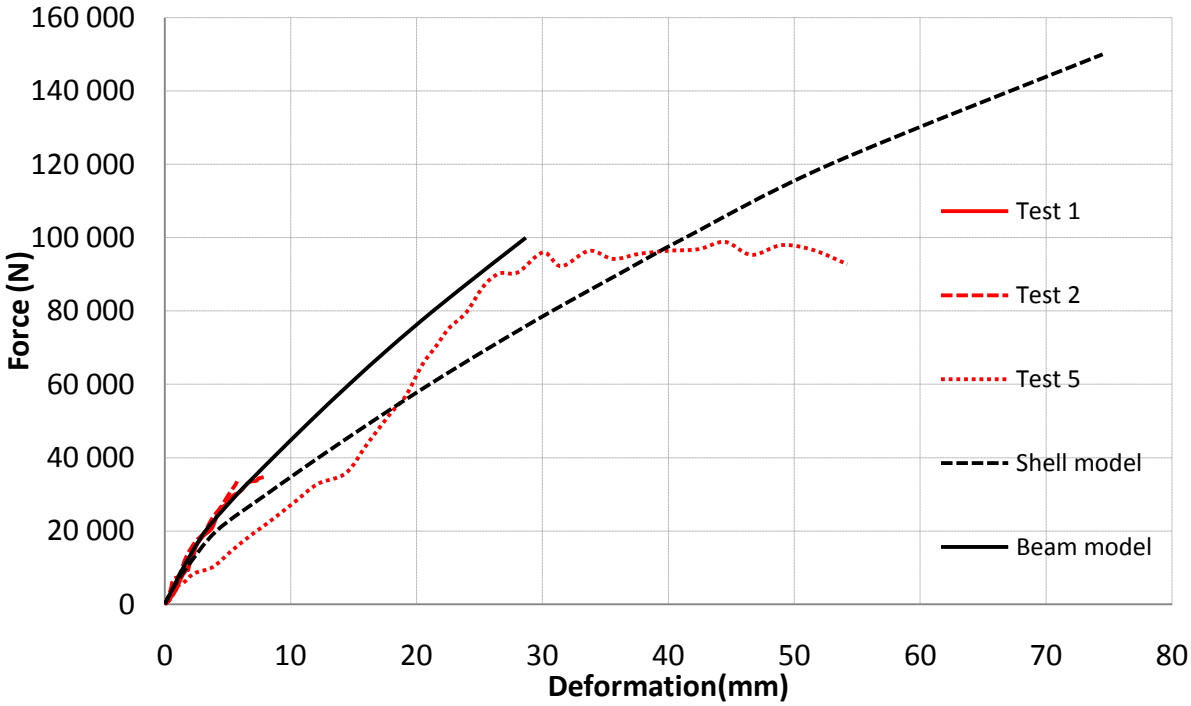

Figure 15a: *Load-slip curve for models and full scale test with a fastener spacing of 200 mm. The deformations are an average of the deformation in Y_1 and Y_2. The test results are from Furulund and Thorrud 2009.*

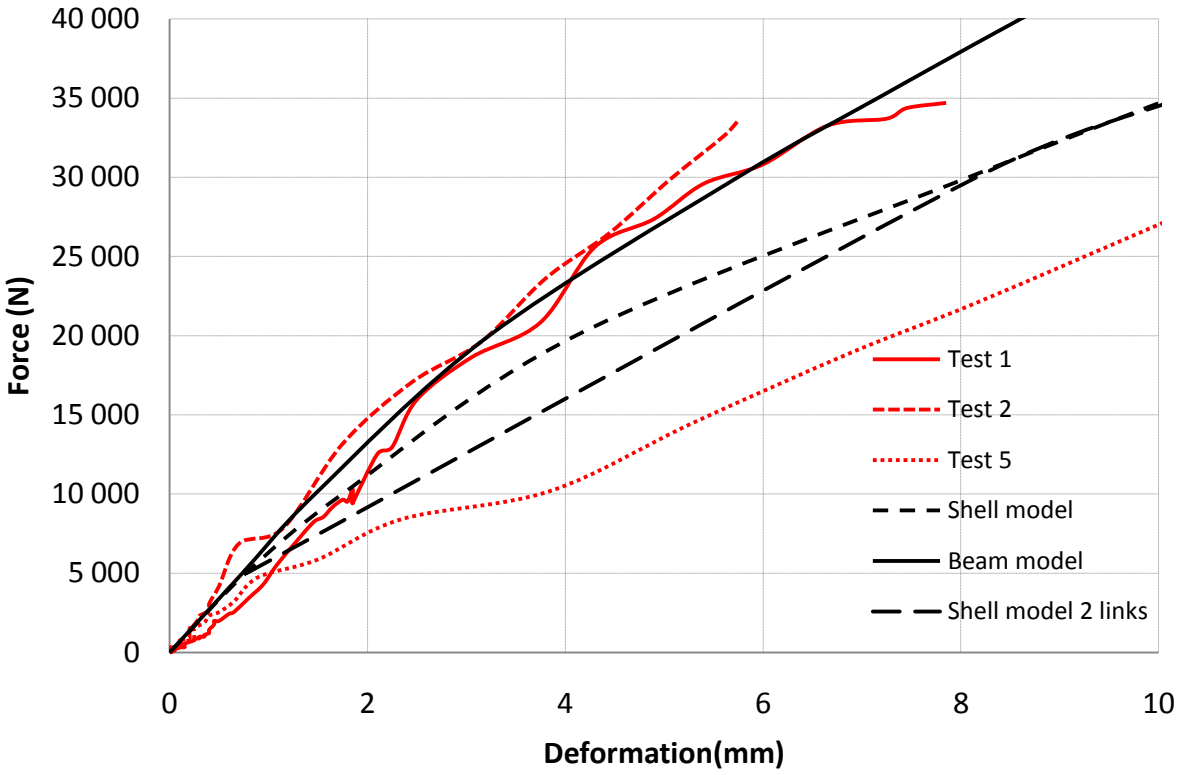

Figure 15b: *Average of Y_1 and Y_2 linear-elastic range. The test results are from Furulund and Thorrud 2009.*

The results show that the analysis models previously described are similar to the test data from Furulund and Thorrud in the linear elastic range (0-35 *kN*). The figures 14 and 15 show that the analysis models give higher deformations compared to the test for the global Y-deformations. The shell model fit the data from test 3 and 4 better than for test 5 for the higher load cases.

The figures 14 and 15 shows that the load-deformation curve for the shell model bends off earlier than the test data while the beam model is similar to the test data. Both of the analysis models continue with the same slope when the test results bend towards failure.

There may be several reasons for test 5 having less stiffness. One may be that the previous tests caused irreversible deformations in the joints, the plywood panel, wood and/or perpendicular to the grain in the GLT frame (A-D and B-C, figure 13). The maximum force in test 4 was 143 *kN* and it is natural to assume that a force of that magnitude causes a irreversible deformation. Therefore test 5 will not be used to validate the deformations of the analysis models, it is only used to show where the experiment reached its ultimate load.

We expected the analysis models to give less deformation than the test, because the fasteners are modeled with independent stiffness in x, y and z-direction.
The manual loading in the full scale test may be an explanation for the stiffness of the test model. The time used to apply the load was different for all the tests in Furulund and Thorrud. The primary loading was applied in 10-50 seconds in all tests. NS-EN 1380 recommends that the time used to apply the load should be 300 seconds ±120 seconds due to the viscoelastic properties of wood. Kollmann and Côtè (1968) strengthen the assumption that the time used to apply load affect the results. If the load is applied too fast the wood will become harder, having less viscous flow deformation. Therefore it is natural to assume that the analysis models would fit the test data better if the load in the test was applied within a correct time interval.

3.2 Link element forces

The link element forces are based on the data from the shell model with 200 *mm* fastener spacing, with an applied load of respectively; 20, 35, 95, 150 and 156 *kN*. The data for the link elements with the highest force is shown in table 2 (shear forces) and table 3 (withdrawal). The respective locations of the link elements with the highest shear force are shown in figure 16.

The link element forces are compared with the ultimate load from Furulund and Thorrud's experiments and the characteristic capacity from EC5. All five link elements used in the model are shown in table 2 and 3; Butt300 and Butt600 are the fasteners in the butt joint between the plywood panels, 300GLT and 600GLT are the fasteners along the model perimeters, between the edge beam and the plywood panel. The number 300/600 describes the distance the link element covers.

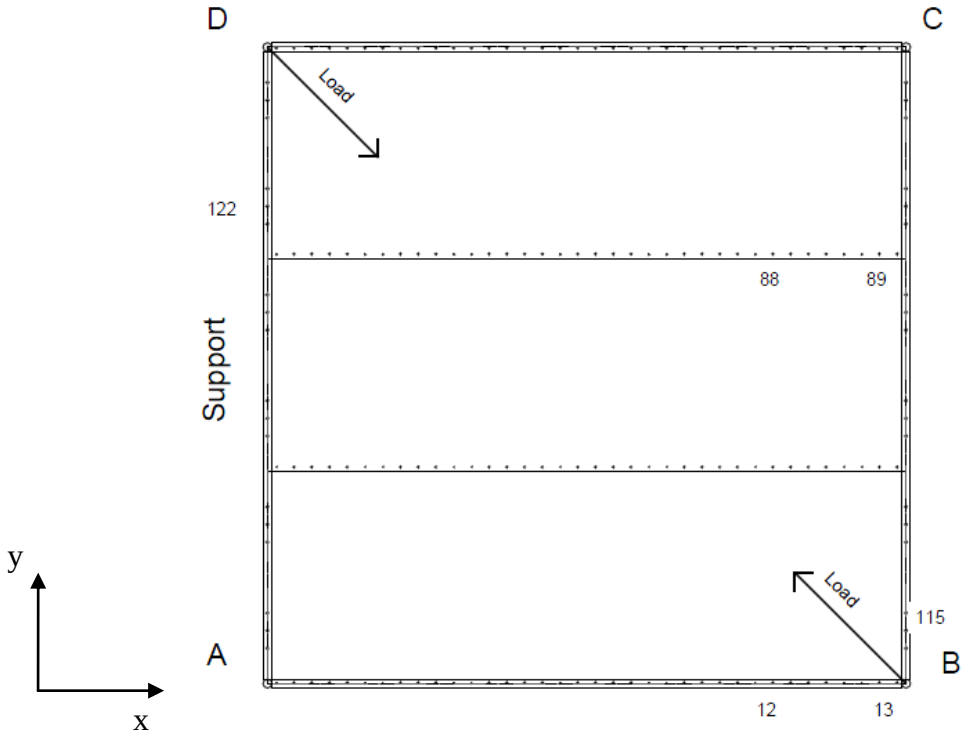

Figure 16: *Placement of the link elements with the highest shear forces*

Table 2: *Link element shear forces with applied forces up to the ultimate load. Analysis model: Shell, 200mm spacing.*

Applied Force	Link	Link element	X-force(N)	Y-force(N)	Shear capacity Test (N)	Shear capacity Eurocode 5 (N)
20 000						
	13	300GLT	668	-676	2 711	1 500
	12	600GLT	1336	-759	5 423	3 000
	89	Butt300	66	-210	2 711	1 500
	88	Butt600	132	-311	5 423	3 000
	122	Gable fastener	-624	2231	18 934	6 450
35 000						
	13	300GLT	846	-722	2 711	1 500
	12	600GLT	1 689	-987	5 423	3 000
	89	Butt300	953	-332	2 711	1 500
	88	Butt600	1 909	-298	5 423	3 000
	122	Gable fastener	1 221	3 165	18 934	6 450
95 000						
	13	300GLT	1 666	-1 086	2 711	1 500
	12	600GLT	3 316	-1 674	5 423	3 000
	89	Butt300	2 029	-500	2 711	1 500
	88	Butt600	4 070	-535	5 423	3 000
	115	Gable fastener	8 037	-7 626	18 934	6 450
150 000						
	13	300GLT	2 469	-1 716	2 711	1 500
	12	600GLT	4 920	-2 445	5 423	3 000
	89	Butt300	2 673	-630	2 711	1 500
	88	Butt600	5 341	-1 089	5 423	3 000
	115	Gable fastener	11 675	12 340	18 934	6 450
156 000						
	13	300GLT	2 198	-1 757	2 711	1 500
	12	600GLT	4 372	-2 483	5 423	3 000
	89	Butt300	0	-323	2 711	1 500
	88	Butt600	0	713	5 423	3 000
	115	Gable fastener	-17 950	12 411	18 934	6 450

Table 3: *Link element withdrawal forces with applied forces up to the ultimate load. Analysis model: Shell, 200mm spacing.*

Applied Force (N)	Link	Link element	Z-force (N)	Withdrawal capacity Test (N)	Eurocode 5 (N)
20 000					
	10	300GLT	-14		6 759
	13	600GLT	-60	-	5 528
	88	Butt300	1	-	6 759
	100	Butt600	13	-	5 528
	104	Gable fastener	372	17 483	10 900
35 000					
	10	300GLT	-147		6 759
	13	600GLT	-191	-	5 528
	88	Butt300	2	-	6 759
	102	Butt600	3	-	5 528
	104	Gable fastener	373	17 483	10 900
95 000					
	10	300GLT	-469		6 759
	13	600GLT	-48	-	5 528
	87	Butt300	-150	-	6 759
	102	Butt600	13	-	5 528
	104	Gable fastener	961	17 483	10 900
150 000					
	10	300GLT	-878		6 759
	13	600GLT	67	-	5 528
	92	Butt300	-312	-	6 759
	102	Butt600	27	-	5 528
	104	Gable fastener	1 410	17 483	10 900
156 000					
	10	300GLT	-1 224		6 759
	13	600GLT	-181	-	5 528
	92	Butt300	553	-	6 759
	102	Butt600	54	-	5 528
	104	Gable fastener	1 759	17 483	10 900

The normal procedure when calculating diaphragm actions in wood panels is to make sure the weak spot in the construction is the fasteners on the panel perimeters, and not the framing or the panels (CEN, 2004). This will make sure the failure mode becomes ductile, if correct fasteners and spacing are used. In test 4, cracks parallel to the grain the edge beam in the gable joint were observed (Furulund and Thorrud, 2009). This indicates that F_v forces cause tension perpendicular to grain (tension perp.) in the GLT. In the analysis models we have observed higher link element forces corresponding to the F_v forces in the outer gable joints.

When using a FE-model to analyze diaphragms it is important to be aware of how the load-slip curves used in the link element will affect the model. The load-slip curves are essentially governed by the type of failure mode. The expected failure mode has to be in accordance with the load-slip data applied in the link element. However, in many cases when structures collapse the failure mode is rather a combination (Bovim, 2011). The key to success is to reveal the dominant failure mode.

The edge beams used in Furulund and Thorrud's tests were highly oversized, compared with edge beams under normal circumstances (Furulund and Thorrud, 2009). Large F_v forces occur due to the stiffness in the weak axis of the edge beams (Bovim, 2011).

The shell model with 200 *mm* spacing seems to underestimate the stiffness both in elastic and inelastic range for global deformation in Y-direction up to 100 *kN* applied load (Figure 15a and Figure 15b). From the load-slip curve used in the single shear connection in the plywood panel butt joint (Figure 8c), we can observe that the analysis curve drops of at approximately 14 *kN* applied load. This is because embedding failure occurs in the joint (Bovim, 2009). When we look at figure 15a and 15b the global load-slip has a clear bend at approximately 20 *kN*. Table 4 shows that the force in the plywood panel joint (Butt 600) is 1324 N at 20 *kN* loading. This means that the sudden bend in the global y-direction (Figure 15a and 15b) can be explained by embedding failure in the plywood panel butt joint.
It could be several reasons for this behavior, one may be that the gable joint in the test act stiffer because some of the F_v forces are absorbed by tension perpendicular in the GLT. The tension perpendicular failure is characterized by small deformation and brittle behavior. Stiffer behavior in the gable joint because of tension perpendicular will unload the fasteners in the plywood panel butt joint and cause later embedment failure.

From table 2 and table 3 we can see the link element with highest force in different load cases. We observe that the gable fasteners transfer a considerable amount of load, both in the horizontal plane and vertically. The ultimate load in the shell model with 200 *mm* spacing was reached at 156 *kN*. At 150 *kN* applied load, the shear force in x- and y-directions in the gable fasteners is respectively; 11 675 *N* and 12 340 *N*. The average ultimate load capacity of the same fastener was 18 934 *N* in the tests. If the gable link element had been modeled as a coupled link element, the fastener would act softer (Chapter 2.4.3) and the F_v force would not unload the fasteners in the plywood panel butt joint to a considerable extent. This shows that the analysis model considerably overestimates the stiffness and ultimate capacity of the gable fasteners.
When the edge beams cross section is halved in the weak axis, failure in the plywood butt joint fasteners occurred at 120 *kN*. This shows that a stiff frame unloads the fasteners.

We observe that the shear force in the link element in the plywood panel butt joint is dominated by the force component in x-direction. The force component in y-direction increases towards the corners of the plywood panels, where it reaches approximately ¼ of the force component in x-direction. The ratio between the x- and y-direction is possibly due to the aspect ratio of the plywood panel.

The shear forces in the x-direction have similar magnitude. This agrees with the failure in test 5 observed by Furulund and Thorrud (2009). The failure appeared simultaneously in all fasteners in the plywood panel butt joint in test 5 (Furulund and Thorrud, 2009).

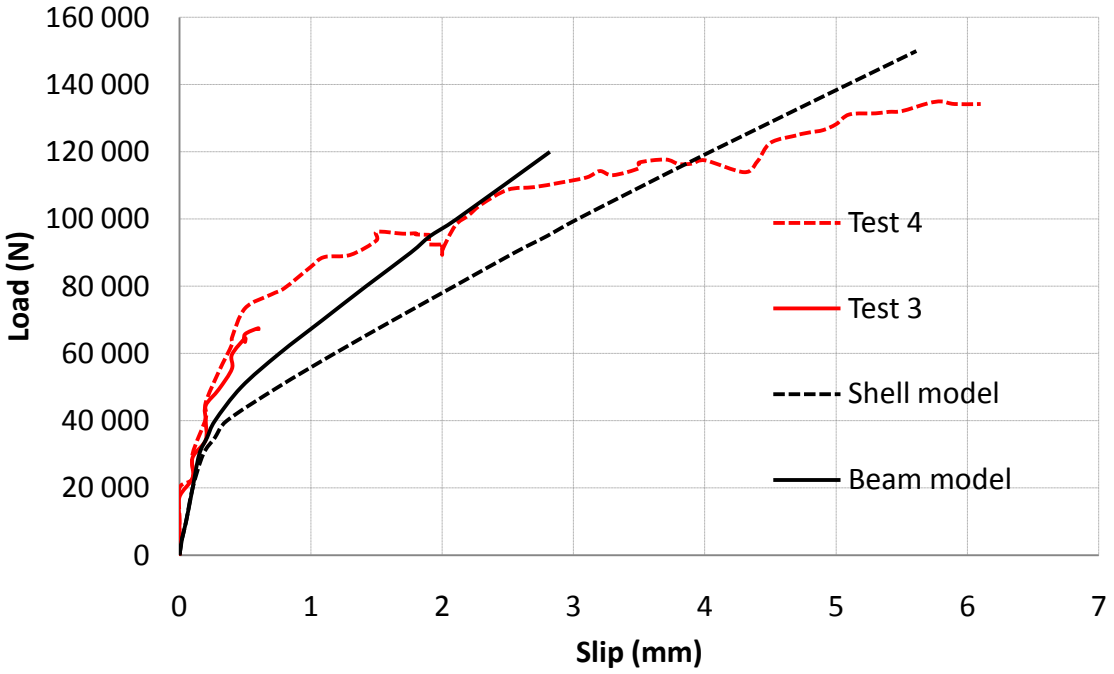

Figure 17: *Load-slip curve for models and full scale test with a fastener spacing of 100 mm. Deformations between the plywood panel and the GLT beam at A-B (ΔX_1).*
The test results are from Furulund and Thorrud 2009.

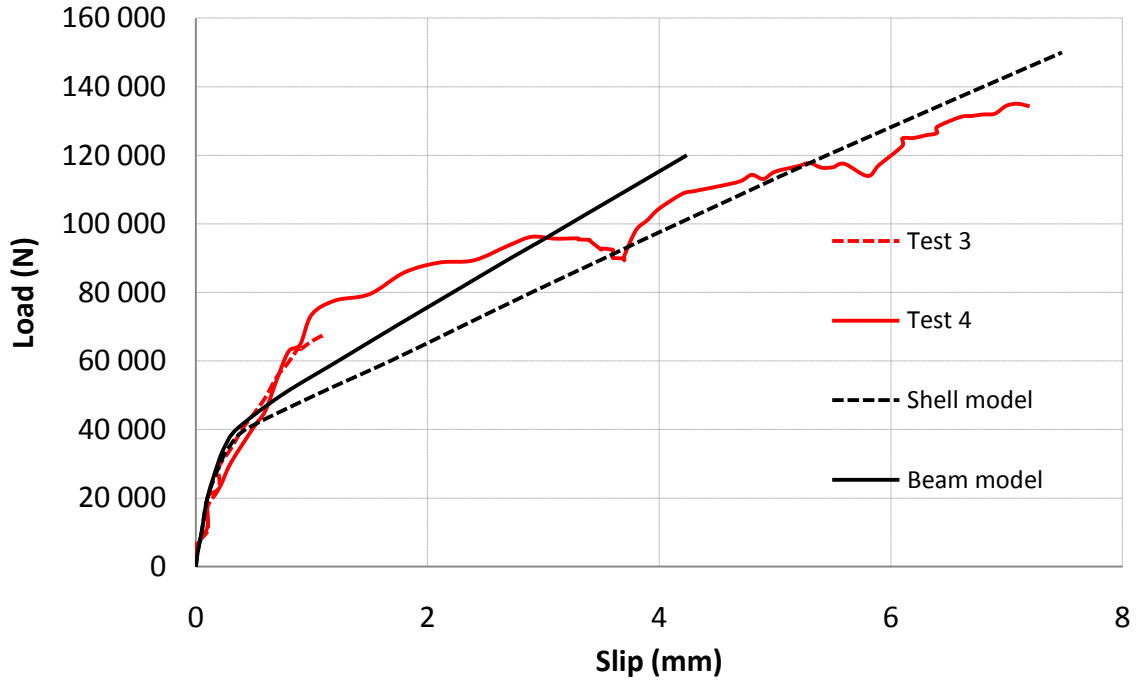

Figure 18: *Load-slip curve for models and full scale test with a fastener spacing of 100 mm. Deformations between the plywood panel and the GLT beam at A-B (ΔX_2). The test results are from Furulund and Thorrud 2009.*

Our study indicates that the fasteners in the plywood panel butt joint are slightly more loaded than the fasteners between edge beam and plywood (Table 2). Figure 17 and figure 18 show that there was considerably more deformation in the joint between the plywood panels than along the edge beam. The reason could be that some of the shear flow is transferred as F_v-force in the roof element profile closest to the corner. This is strengthened by the higher F_v forces in the gable link elements closest to the corners.

The load-slip curve for shear capacity of fasteners plywood-to-edge beam is not entirely correct, since the same data as for fasteners in the plywood butt joint is used. The plywood-to-edge beam fasteners on the perimeter of the edge beam have a 15 *mm* longer anchor length, because the fastener in the panel goes 15 *mm* through the butt joint. A correction of this would have some effect in making the model stiffer globally.

In our study we have tried to give the single spring configuration coupled properties by adding hinges at the dummies that is connected with the link elements. The link elements were hinged in the xy-plane at both sides. The hinges do not seem to work properly. At small rotations the program seems to ignore the hinges and the result from calculations are equal with and without the hinges. This means that only stiffness in one direction is provided. When the hinged configuration was tested on the gable fasteners, the computation failed. Apparently combining hinges and the multi-linear elastic spring in SAP2000 does not work and causes instability in the stiffness matrix.

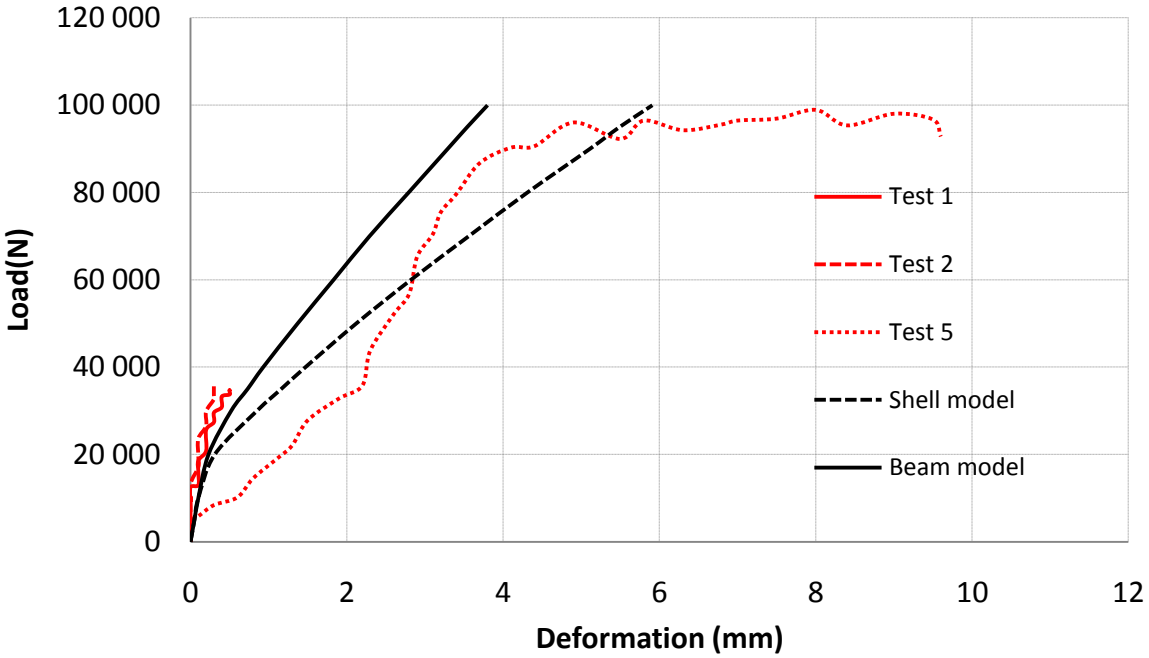

Figure 19: *Load-slip curve for models and full scale test with a fastener spacing of 200 mm. Deformations between the plywood panel and the GLT beam at A-B (ΔX_1). The test results are from Furulund and Thorrud 2009.*

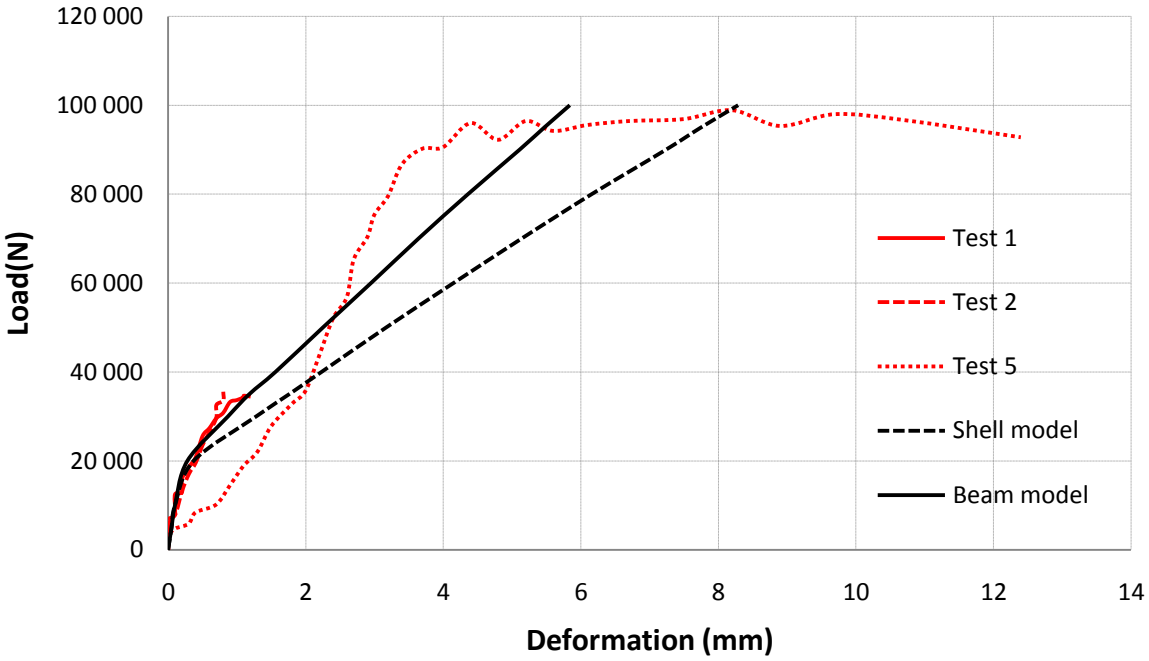

Figure 20: *Load-slip curve for models and full scale test with a fastener spacing of 200 mm. Deformations between the plywood panel and the GLT beam at A-B (ΔX_2). The test results are from the test done by Furulund and Thorrud 2009.*

3.3 Meshing and link element distance

To investigate the effect of meshing we halved the size of the shell elements. The link element distance was doubled and halved, to respecetively 300 *mm* and 1200 *mm* to investigate how lumping affect the deformations. The results are shown in figure 21.

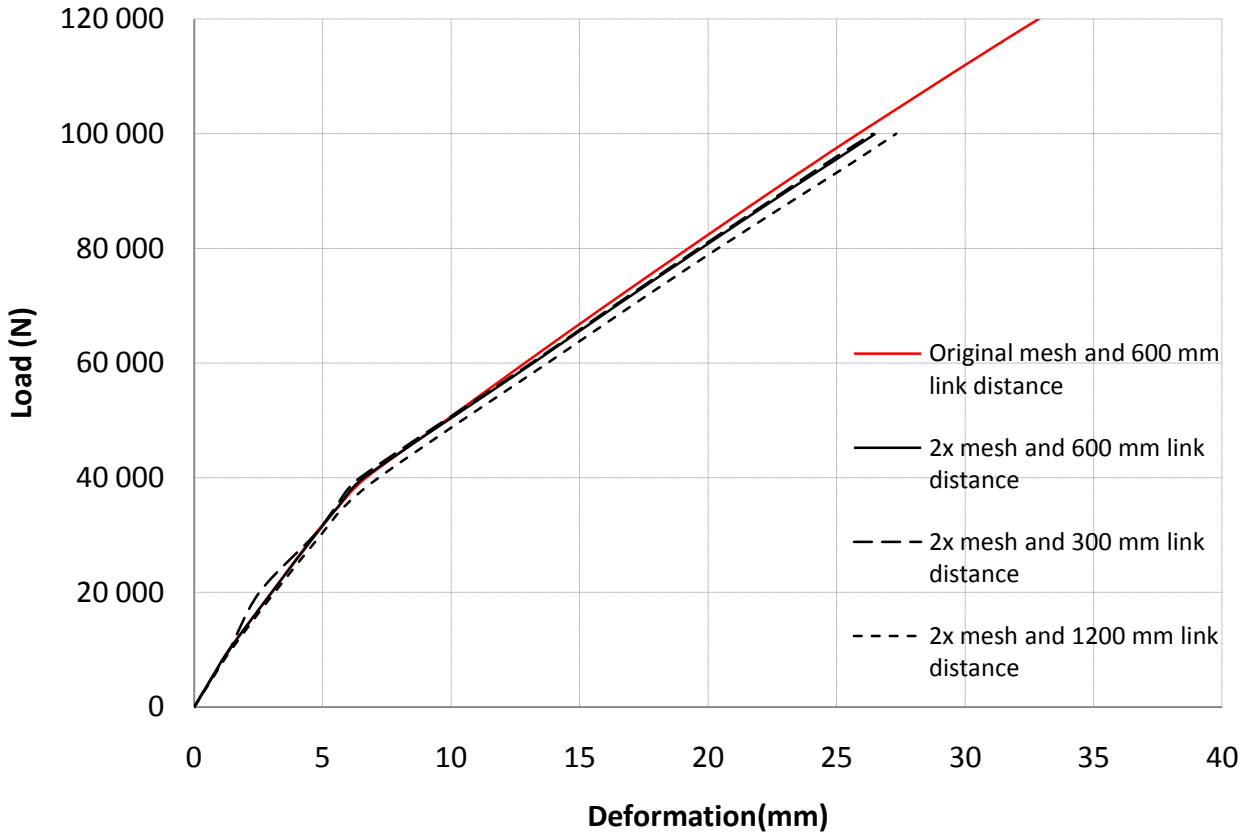

Figure 21: *Load-slip curve for shell models with different meshing and link element distance, to view the effect. The deformations in Y-direction are measured in Y_1 and Y_2.*

Figure 21 shows that the deformations of the shell model are slightly affected by mesh size. This coincide with the results from Erichsen et al (2007). It was expected that the mesh size would affect the deformations in some degree due to the decrease in aspect ratio. The wood rows have an aspect ratio of 12,5. As mentioned in chapter 2.6 CSI Berkeley does not recommend an aspect ratio higher than four and absolutely not higher than ten for shape purposes. Although the aspect ratio is too high it does not seem to influence the results.

The results from the link element distance comparison (Figure 21) show the result same as for the mesh size, at least for the global deformations. The global deformations are slightly affected by the link element distance when the distance is doubled and halved to respectively 1200 *mm* and 300 *mm*.

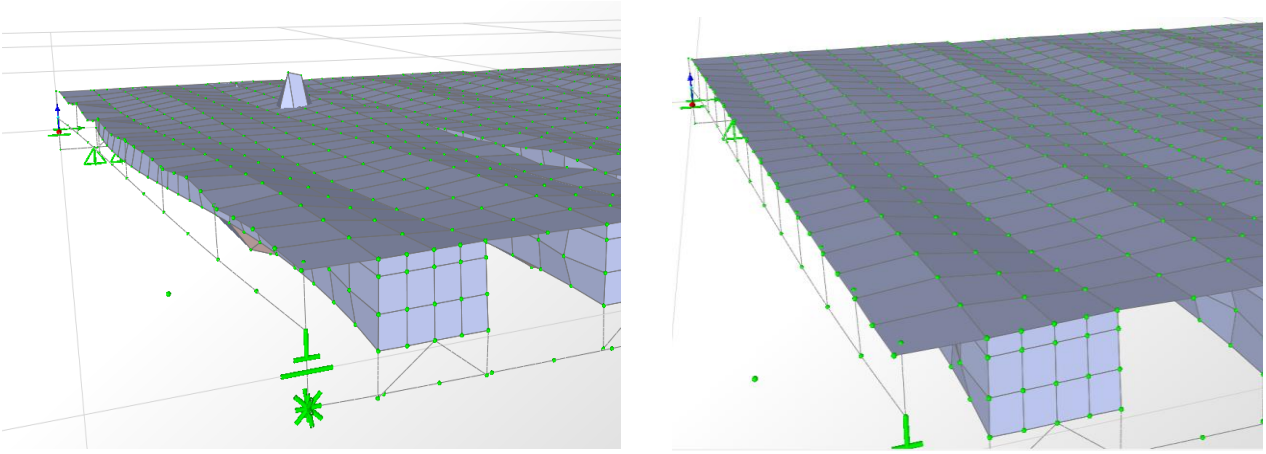

Figure 22: *Buckling behavior for the shell model, with respectively 1200 mm link element distance to the left and 600 mm link element distance to the right. Applied load is 70 kN and 2x mesh. The deformation scaling factor is 25, to amplify the deformations.*

For the local deformations, the link element distance had the effect of, more buckling behavior of the plywood panel when the link element distance was increased (Figure 22). This is probably due to the magnitude of the forces in the links element when that many fasteners are lumped together and the lack of support to the plywood panel when the distance is 1200 *mm*.

This show that the lumping used in the analysis models is correct.

3.4 Shell stress distribution and buckling behavior

Shell stress distribution can be viewed in SAP2000, figure 23a and figure 23b show the panel shear stress distribution in the plywood (σ_{xy}) for the beam and shell model. Figure 24 shows the panel shear in the metal sheeting viewed in 3D.

During the modeling we observed buckling of both the metal sheeting and the plywood panel. The buckling of the plywood panel is shown in figure 22, for the shell model with 1200 *mm* link distance and 600 *mm* link distance. The buckling in the metal sheeting is primarily observed in the bottom of the element cross section (Figure 25). Both upwards buckling and downwards buckling appear.

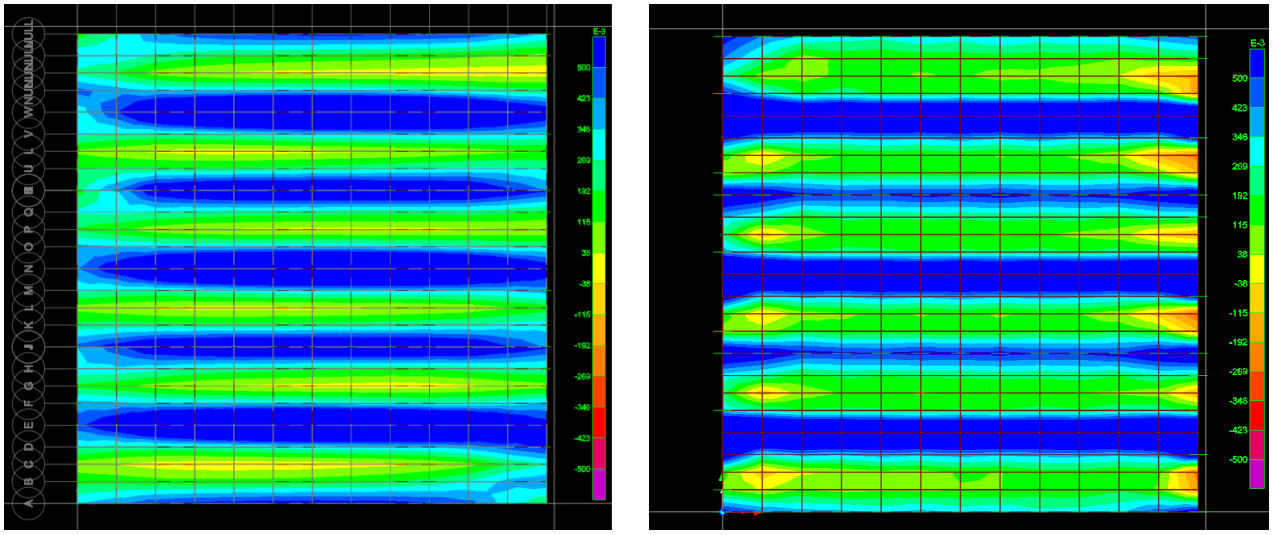

Figure 23a (left): *Panel shear stress (S12 = σ_{xy}) in the plywood panel for the beam model.*
Figure 23 b(right): *Panel shear stress in the plywood in for the shell model.*
The applied load is 95 kN.

One of the advantages of using three-dimensional FE-software with shell elements is the possibility to observe the stress distribution in the light weight roof elements. Hopefully this possibility will help Larvik Lett-Tak optimize their analysis procedure, by being able to observe the stress in critical points of the light weight roof elements further. In particular being able to observe the shear stress distribution in the sheeting metal and the wood rows of the elements is a big step for Larvik Lett-Tak's analysis process (Bovim, 2011). Figure 23 and 24 show that the shear stresses are distributed, along the perimeter of the plywood panels and in the middle of the plywood panels. The shear flow is a result of the forces in the element profiles and frames connected to the elements. Figure 23a and 23b show that the panel shear stress in the plywood panel above the metal sheeting is relatively low compared to the other part of the plywood panel. The buckling behavior observed in the metal sheeting may be a

result of torsion forces in the metal sheeting (Bovim 2011). Rindal (2009) purposed that the metal sheeting, wood ribbon and plywood panel interact as a torsion box. This may be the reason for the stress being lower above the metal sheeting. The shear forces in the torsion box counteract the shear flow along the plywood panel for this case. If the forces in the torsion box had an opposite sign it would make the stress above the element profiles even higher. The shear flow along the sides is lower than the stress between the plywood panels (figure 23). This is most likely because the F_v forces are transferred by the link elements in the gable closest to the corners. The link element forces in x-direction (F_v) are considerably larger in the corners compared to the F_v forces in the middle of the model.

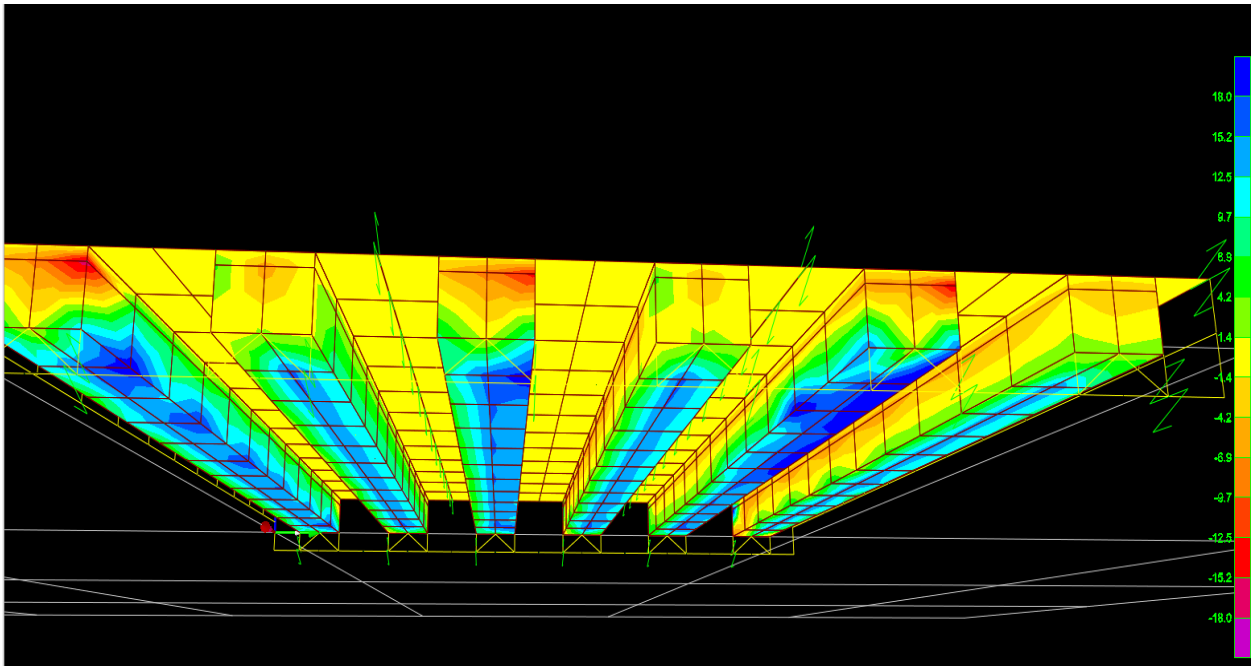

Figure 24: *Shell shear stress in the metal sheeting plywood panel and wood ribbon for the shell model, viewed in 3-D. Applied load is 95 kN.*

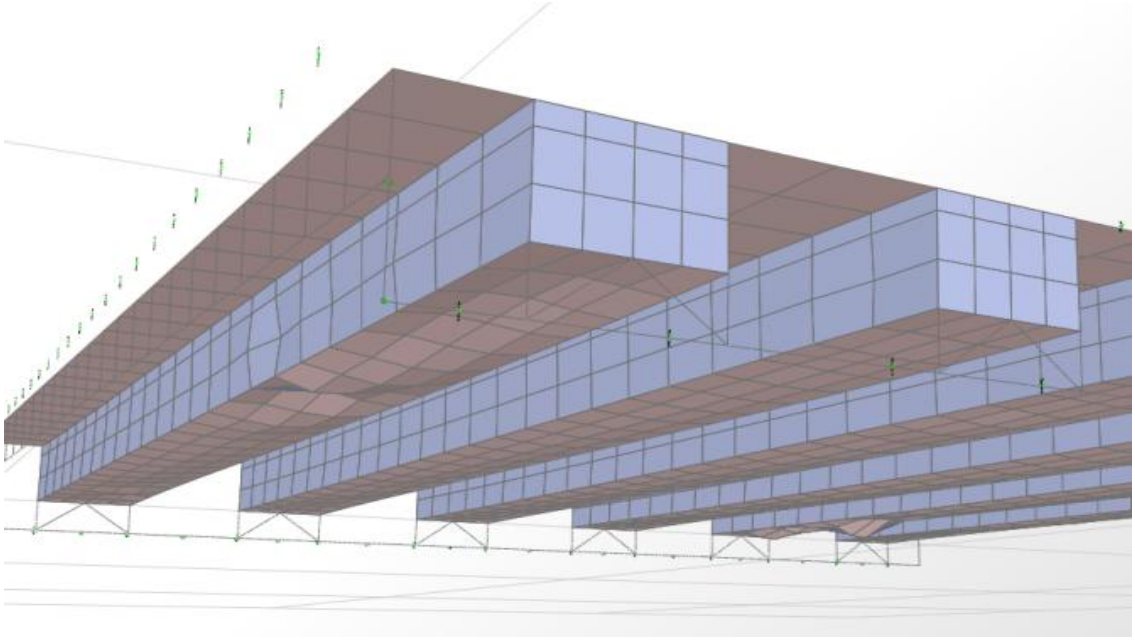

Figure 25: *Buckling behavior of the metal sheeting. Applied load is 80 kN, and the deformation scaling factor is 10. Shell model with 2x meshing.*

3.5 Torsion stiffness

The torsion stiffness of the light weight roof element is calculated in accordance with Rindal (2010), more details about the calculations are shown in appendix D. The results are shown in table 4. The theoretical model and the focus 2D model used in table 2 are developed by Rindal.

Table 4: *Rotations due to moment about the x-axis of the light weight roof element section. Details about the element setup are shown in appendix D.*

Model:	**Moment (*Nmm*)**	**Rotation (˚)**
Theoretical	2 748 534	1
Focus 2D	2 748 534	1,0004
Shell model	2 276 283	1,55
Beam model	2 276 283	6,87

The shell model and the simplified analysis model from Eli B. Rindal (2010) have similar rotation values (Table 4), though the shell model has more rotation. The beam model's torsion stiffness is too low, the rotation is more than six times as high as for the other models.
It is hard to conclude whether the shell model or the model purposed by Rindal is correct with respect to torsion stiffness. The fact that they are similar implies that they are within the correct range. Due to the simplifications in Rindal's model and the shell models similarity to the test results from Thorrud and Furulund it is natural to assume that the shell model is more accurate.
The beam model does not have sufficient rotation stiffness, probably due to the nature of the non-prismatic beam element. It seems as though the beam sections shown in figure 4 should have been modeled as closed sections to achieve sufficient torsion stiffness. On the other hand if the beam model had higher torsion stiffness it would be an even worse fit for the test data due to the stiffness. This implies that the beam model should have had another configuration with respect to the dummies. The dummies should have been hinged so that they do not transfer moments and unload the metal sheeting at the supports.

3.6 Uplift deformations

As previously described there is a 6 *kN* (-Z) force in corner C (Figure 13). To simulate the uplift deformations a model without constraint at C has been made, with and without the 6 *kN* force in C. The weight in C is hard to estimate, as there is no data documenting the magnitude. When comparing the models with Furulund and Thorrud's results we assumed that there was no uplift until 135 *kN* load, due to the uncertainty in the weights and uplift deformations. Hence there is a roller restraint in C in this study, except when modeling the uplift forces explicitly.

Furulund and Thorrud observed that the weights in C counteracted the uplift forces until the applied load reached 135 *kN*, then the uplift changed from zero to about 350 *mm* at 143 *kN*. Although Furulund and Thorrud did not observe any uplift before 135 *kN* loading it is natural to assume that there was some degree of uplift deformations earlier. The results are shown in figure 26. The uplift effect occurs in both of the analysis models.

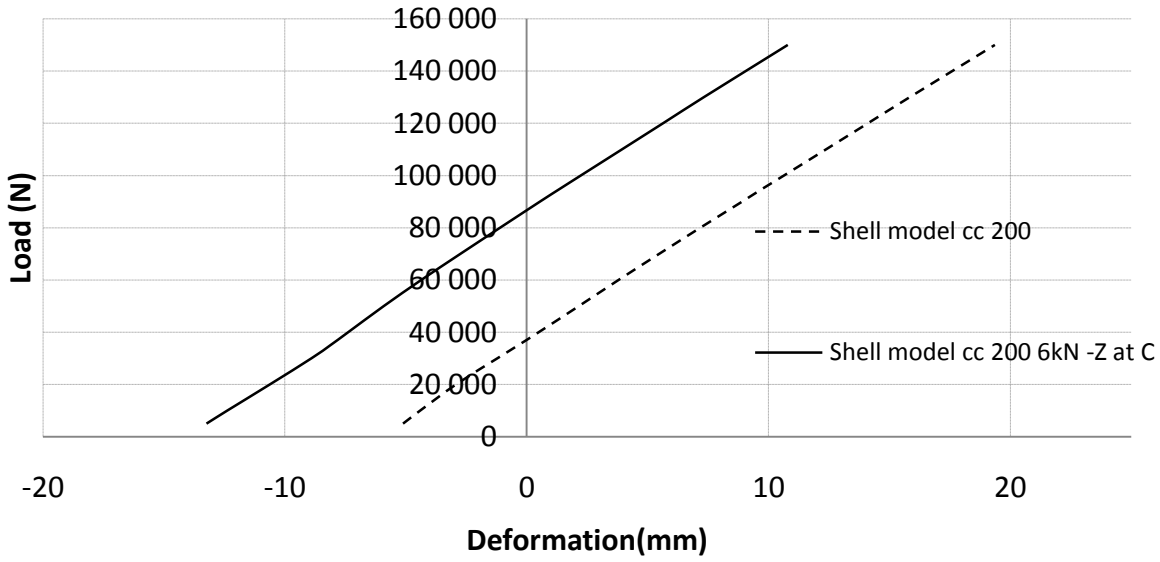

Figure 26: *Load-slip curve for z-direction in corner C with and without a 600 kg weight in C. Tested on the shell model with a fastener spacing of 200 mm.*

Figure 26 shows that the uplift deformation when C is not restrained increases linearly when the applied load increase. The uplift forces are a result from the eccentricity moment due to the F_h forces. Although the uplift deformations in the analysis models are smaller than the uplift deformations in the tests, the test results show that the effect is taken into account.

3.7 Computation time

We have compared the computation times for the analysis models, with different mesh, fastener spacing and link element distances, to see what influences the time used. The computations are done with 70 *kN* load and shown in table 5. The values are dependent on memory and speed of the computer solving the equations, therefore the values will not be the same for other computers. The values are used to show a tendency, not to give exact value.

The computation time is an important factor when modeling larger buildings and structures. This could be a limiting factor for the applicability of FE-models.

Table 5: *Computation time for the models in this study. Comparing link distance, mesh size, fastener spacing and number of nodes.*

Model	Fastener spacing (*mm*)	Link Distance(*mm*)	Mesh	Nodes	Time(s)	Time/node
Beam	100	600	-	597	7	0,012
Beam	200	600	-	597	6	0,010
Shell	100	600	-	943	11	0,012
Shell	200	600	-	943	11	0,012
Shell	100	600	2x	2 314	27	0,012
Shell	100	300	2x	2 410	30	0,012
Shell	100	1 200	2x	2 302	26	0,011

As shown in table 5 the analysis of the beam model is fastest, with the shell model being 2-3 seconds slower. The meshing seems to influence the computation time, when increasing the meshing two times the computation time increases with about 20 seconds. This is natural because it causes an increase in the number of nodes. Table 5 shows that there is a close relation between computation time and the number of nodes.

The beam model has 597 nodes, when modeling a 50 x 60 m roof the number of elements would be 160 and the number of nodes would be 31 840. For the shell model with 2x meshing the number of nodes would be about 122 660. A simulation of the model with 122 600 nodes would take about 24 minutes, this shows the importance of using a suitable mesh and minimizing the number of nodes.

The number of links seems to have less influence on the computation time, despite the non-linear behavior of the link elements.

5. Conclusion

The analysis models are not fully verified in this study. The shell model is close to verification with the correct fastener configuration in the gables the shell model is most likely to have a ultimate load closer to the tests. The beam model was made with an error, which was discovered late in the process, therefore the data has been presented and the model has not been modified.

The analysis models clearly show that the F_v and F_h forces have a considerable magnitude as purposed by Furulund and Thorrud. Link elements with coupled behavior are essential to properly transfer these forces, due to the magnitude and direction of the forces.

With a proper link element in the gable the shell model gives Larvik Lett-Tak the possibility to observe realistic diaphragm action in the plywood panel, due to different horizontal load cases. The link element forces shows which fasteners are the critical point in the structure. In the shell model critical stress and buckling of the metal sheeting can be observed and measured.

The shell model may most likely be used to study the effects of vertical loads on the light weight roof elements.

The models developed in this study will be of great value as a base for simulating small scale tests and other scientific study of the light weight roof elements. Being able to observe distribution of forces within all components of the light weight roof element is important for further understanding and developing of the light weight roof element.

6. Further work

There are several parts of the model that needs to be investigated further and other perspectives to be viewed.

Fasteners

As previously described the link elements used in this study has uncoupled behavior, one of the first steps in making the FE-models more accurate should be to implement the coupled behavior of the fasteners. The effect of tension perpendicular in the gable joint has to be further investigated. In addition more fastener data should be tested:

- Shear action between plywood and glue laminated timber.
- The interaction between the sheeting metal and the GLT in the gable of the element when there are negative z-forces present.
- Shear and withdrawal data for shot nails. To simulate the interaction between edge beams of steel and the light weight roof element.

TEKLA Structures

Larvik Lett-Tak want to explore the possibilities of BIM and 3D-modeling, using SAP2000 and TEKLA Structures. In this relation the interaction between TEKLA Structures and SAP2000 should be investigated. There is a possibility in TEKLA Structures to export models to SAP2000 but the level of detail and compatibility has not been investigated.

The beam model

This thesis has shown that the non-prismatic beam element in the beam model has to be developed further. The current non-prismatic beam element does not have sufficient torsion stiffness. In addition the possibility of making a less detailed model should be investigated, with fewer nodes and thereby less computation time.

Super element:

One approach to model large roofs with light weight roof elements and less computational time is to use superelements. The superelement method especially fits for structures containing similar parts (Bell, 1994). We think this approach should be paid further attention.

8. References:

BELL, K. 1994. *Matrisestatikk.*

BOVIM, N., I. 2009. *Skivekonstruksjoner med Lett-Tak-elementer*. Unpublished work. 12 pages

BOVIM, N., IVAR. 2011. *Master of science, Amanuensis II. Lectures and advice about statics and wood structures.* Institute for Mathematics and Technical Science, the Norwegian University for life Science.

CEN. 2004. EN 1995-1-1. *Eurocode 5: Design of timber structures. Part1-1: General-common rules and rules for buildings*. Brussels. 123 pages.

CEN.2009. *EN 338. Structural Timber- Strength classes*. Brussels. 10 pages.

CSI 2011a. *CSI Analysis manual Reference Manual For SAP2000, ETABS, SAFE and CSiBridge.* Computers and Structures, Inc. 494 pages.

CSI, B. 2011b. *CSI WIKI* [Online].

DAHL, K., BERBOM. 2009. *Mechanical properties of clear wood from Norway spruce.*

ERICHSEN, H., TORE., BOVIM, N., IVAR. & SIEM, J. 2007. *Forankring av avstived skivekonstruksjoner av tre og trebaserte materialer*. FOU-programmet "Klima 2000". Oslo. 33 pages.

FELIPPA, C., A. 2004. *Introduction to Finite Element Methods*, Department of Aerospace Engineering Sciences and Center for Aerospace Structures University of Colorado.

FURULUND, E., M., & THORRUD, K. 2009. *Roof diaphragms with lightweight structural elements.*, Norwegian University of Life Science.108 pages.

GIRHAMMAR, U., A., BOVIM, N., I. & KÄLLSNER, B.2004 *Characteristics of Sheathing-to-Timber Joints in Wood Shear Walls*. 6 pages.

HUEBNER, K., H., DEWHIRST, D., L., SMITH, D., E. & TED, B., G. 2001. *The Finite Element Method for Engineers*, John Wiley & Sons, Inc. 720 pages.

JUDD, J., P. 2005. *Analytical Modeling of Wood-Frame Shear Walls and Diaphragms.* Master of Science Birmingham Young University.262 pages.

KOLLMANN, F., P,FRANZ & CÔTÈ, A., WILFRED 1968. *Principles of Wood Science and Technology ch 2,6 & 7*, Pensumtjeneste A/S.

LARSEN, J.-F. 1975. *Lättbärverk med samverkande blandkomponenter.* Stockholm, SWE.

LETT-TAK, S. A. 2011. *www.lett-tak.no* [Online].

RINDAL, E. B. 2010. *3D-Modeling of lightweight roofelements.* Master, Norwegian University of Life Sciences.86 pages.

SCHUELLER, W. 2008. *Building Support Structures Analysis and Design with SAP2000 Software,* United States of America, Computers and structures Inc. 613 pages.

SINTEF BYGGFORSK. 1996. *Teknisk Godkjenning: Finnforest spruce konstruksjonskryssfiner*. *In: Ø*.RAMSTAD, T. (ed.). Oslo: Norges byggforskningsinstitutt.

SINTEF BYGGFORSK. 2000. *Teknisk Godkjenning Lett-Tak eakelementer*. Oslo: Sintef Byggforsk formerly known as NBI.

VESSBY, J., SERRANO, E. & OLSSON, A. 2010. *Coupled and uncoupled nonlinear elastic finite element models for monotonically loaded sheathing-to-framing joints in timber based shear walls*. Engineering Structures, 9 pages.

WILSON, E., L. 2004. *Static and Dynamic Analysis of Structures. A physical approach with emphasis on earthquake engineering. Fourth ed.*: Computers and Structures, Inc. 380 pages.

Electronic attachments:

0: The Master thesis

- Master_martin_kleven_roald_norås.pdf

1: FE-models with model description

- Beam model 100.SDB
- Beam model 200.SDB
- Shell model 100.SDB
- Shell model 200.SDB
- Shell model 100 2x 300.SDB
- Shell model 100 2x 600.SDB
- Shell model 100 2x 1200.SDB
- Shell model 100 uplift.SDB
- Shell model 100 uplift 6 kN.SDB
- Shell model 2 links.SDB
- Section beam.SDB
- Section shell.SDB
- Model description.docx.

2: Results

- Results.xlsx

3: Fastener data:

- Load-slip curves and corresponding data. (inndata.xlsx)

4: An analysis example from Larvik Lett-Tak A/S by Nils Ivar Bovim: Sandved_Arena Nils Ivar Bovim.pdf

5: Experiment data from Furulund and Thorrud:

- Skivekonstruksjoner med Lett-Tak-elementer - 2009 -Thorrud og Furulund.pdf

- Data fra testing av enkeltforbindere:

- Finér-Finér
- Stål-limtre
- Uttrekk

- Data fra testing av Lett-Tak-elementer

- 310 mm elementer.xls
- 210 *mm* elementer.xls

APPENDIX:

Appendix A: A detailed description of the modeling process

This is an appendix to the thesis by Kleven and Norås (2011). The making of the FE-models in the thesis will be described here, the objective is to make it possible to recreate the FE-models later. This appendix is a supplement to the thesis. The SAP2000 reference manual (2011) is basis for most of the information about the elements in SAP2000. In addition Wilson (2004) and Schueller (2008) have been used for further explanation about the specifics of the elements. FE-theory has been used as a supplement to understand the element configurations better.

All of the materials in the model are created manually, to match the values from Furulund and Thorrud and to have the orthotropic properties of wood. The material data used in the FE-models are shown in appendix B.

1. Grid

The grid setup of the model is of great importance when modeling in SAP2000, our grid is based on the element size (7,2 m x 2,4 m). Thereby the gridline spacing is 600 *mm* in x-direction. In y-direction the spacing is based on the setup of the gable, to make it easy to connect the GLT beam to the light weight roof element. The spacing changes from 300 to 100 *mm* in y-direction.

The z-direction of the grid is based on the height of the element and the distance from the neutral axis of the GLT beam to the bottom and top of the element. There are some differences in the grip setup for the beam model compared to the shell model for practical reasons. The grid is changed when modeling the links, this will be described in the chapter 4. The basic grid of the models is shown in table 1. The models are shown in figure 1.

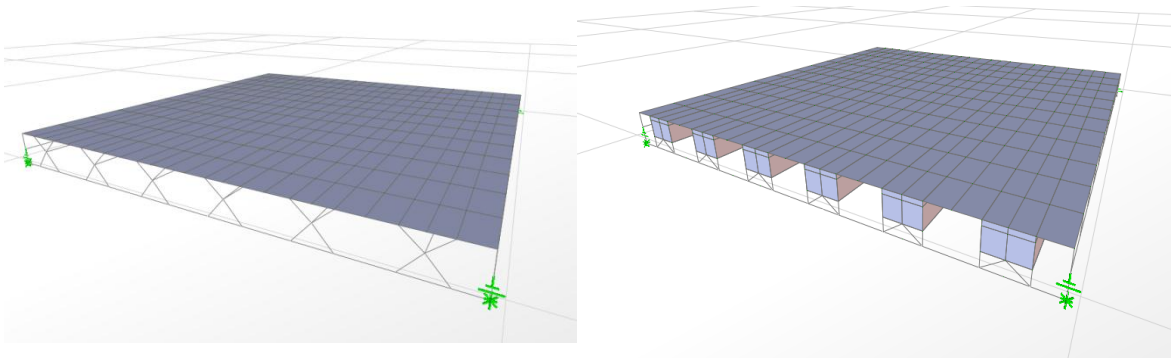

Figure 1: *Left: Beam model in viewed on 3D. Right: Shell model viewed in 3D.*

Table 1: *The basic grid setup used in the shell model and the beam model.*

X-Grid data	Ordinate
A	0
B	600
C	1200
D	1800
E	2400
F	3000
G	3600
H	4200
I	4800
J	5400
K	6000
L	6600
M	7200

Z-grid data	Ordinate
Z1	-202,5
Z2	-135
Z3	0
Z4	310
Z5	381

Y-Grid data	Ordinate
1	0
2	335
3	600
4	865
5	1200
6	1535
7	1800
8	2065
9	2400
10	2735
11	3000
12	3265
13	3600
14	3935
15	4200
16	4465
17	4800
18	5135
19	5400
20	5665
21	6000
22	6335
23	6600
24	6865
25	7200

2. Frame elements

There are several frame elements in the FE-models, the GLT framing, the dummy elements and the non-prismatic frame element of the beam model. The GLT frames and the non-prismatic frame element are made using the section designer, because there are no predefined elements with adequate properties. The non-prismatic frame element is a combination of two frame elements made in the section designer (figure 2). The frame section between the support ends of the roof elements and the end section of the roof element. The two elements are combined using the non-prismatic frame option, with the end section in the end and the other element between the ends.

The GLT frame are also made with the section designer, the insertion point is set to the neutral axis, although it is possible to change it to the top of the frame where the light weight roof element is connected to the frame. Instead dummies have been used to connect the GLT frame to the light weight roof elements. The dummies are made to be stiff but not to an unrealistic degree. Using a standard steel section and multiplying the stiffness values by 100 and the mass and weight properties with 0. Making it weightless and stiff, transfering the forces without significant deformations.

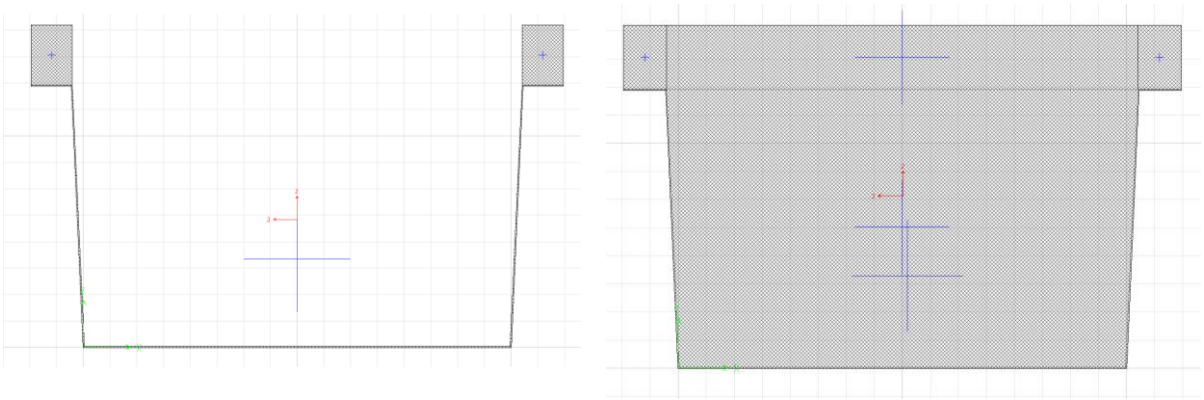

Figure 2: *Left: Cross section made using the section designer option. The light weight roof element modeled as a beam element. Right: The end-section of the beam element modeling the light weight roof element.*

3. Shell elements

The shell elements used in the model are modeled with thin shell options except the wood rows of the light weight roof element, which has thick shell options. The shell elements used in the beam model are the plywood panels at the top with the properties from Furulund and Thorrud. In the shell model there are more shell elements, the metal sheeting, the wood rows, the end plate, and the wood ribbon at the end of the light weight roof element. To make the modeling of the shell model possible the grid was changed to correspond with the perimeters of the specific shell elements.

4. Link Elements

The link elements used have non-linear properties and non-linear load-slip curves from Furulund and Thorrud.

The fasteners between the plywood panels and the fasteners between the plywood panel and the GLT beam are modeled with the same force-deformation curves for shear forces. The withdrawal forces are calculated separately for the two fastener types. The modeling of the links between the plywood panels is complex, to make it easier there is a 4 *mm* gap between the two plywood panels. There are two beam elements connecting the plywood panels, with a link element connecting the beam elements together. The link element has zero length and thereby it has to be modeled using the interactive database interface. The node connecting the two beam elements together is disconnected and the node label is noted. The nodes are the start and end nodes of the link element.

The same procedure has to be done for all of the links. Along the length of the elements the plywood panels are connected to the GLT beam. There are two plywood shells and one dummy connected, they have to be disconnected. Then the shell elements are merged together to one node before the link element is connected between the shell elements and the dummy.

The link elements connecting the end of the light weight roof element to the GLT beam at the end has two different setups. The reason for the two setups is the direction of the z-forces, the experiment data was for withdrawal of screws hence it is not tested for negative z-forces. The link elements with negative forces are thereby fixed in the z-direction. The shear force-deformations are the same in both link elements. In the gable there are four beam elements joint together where the link is connecting the dummies to the GLT beam. Hence the four elements have to be disconnected. Then the GLT beams have to be connected in one node and

the dummies in another node. The link element is then connected between the two elements using the interactive database.

All of the link elements are fixed in the rotational DOFs

Appendix B: Material input data to SAP2000

A transverse isotropic behavior of solid wood and GLT is assumed, this correspond to an orthotropic behavior where two off the planes are equal. The difference between elasticity modulus in radial (E_{RR}) and tangential (E_{TT}) is relative small compared with longitudinal (E_{LL}) direction in solid wood and GLT, so this simplification is passable. The orthotropic compliance matrix is thereby reduced to 5 independent elastic constants (Dahl, 2009) for a transverse isotropic material (figure 1). Since choosing a transverse isotropic behavior is not an option in SAP2000, this is achieved by not distinguishing between the parameters in the XY-plane.

$$\left[S_{ijkl}\right] = \begin{bmatrix} \frac{1}{E_{LL}} & -\frac{\nu_{LP}}{E_{LL}} & -\frac{\nu_{LP}}{E_{LL}} & 0 & 0 & 0 \\ & \frac{1}{E_{PP}} & -\frac{\nu_{PP}}{E_{PP}} & 0 & 0 & 0 \\ & & \frac{1}{E_{PP}} & 0 & 0 & 0 \\ & & & \frac{1+\nu_{PP}}{2 \cdot E_{PP}} & 0 & 0 \\ & sym & & & \frac{1}{G_{LP}} & 0 \\ & & & & & \frac{1}{G_{LP}} \end{bmatrix}$$

Figure 1: *Stiffness matrix for a transverse isotropic material Dahl(2009).*

With:

E_{LL}= Longitudinal elasticity modulus = E_1.

E_{PP} = Perpendicular elasticity modulus = E_2 = E_3.

G_{LP} = Shear modulus = G_1 = G_2 = G_3.

ν_{LP} = in plane Poisson's ratio.

ν_{PP} = out of plan Poisson's ratio, corresponding to the RT-plane in wood.

The elastic parameter used for the GLT and solid wood is based on mean values which are used by Larvik Lett-Tak for static analysis. For ν_{LP} and ν_{PP} we have chosen the value; 0,1. Deciding the exact for Poisson's ratio is not a straight forward procedure. And since the value is not essential in our case, this is not further investigated. The density of the plywood and GLT used were measured by Furulund and Thorrud.

Plywood is treated as an orthotropic material due to the three orthogonal symmetry planes in a 5-ply system such as Wisa Spruce plywood. E_1 and E_2 are given in the technical approval for Wisa plywood made by Sintef Byggforsk. They have set EA_0 and EA_{90} to respectively108 *kN/mm* and 77 *kN/mm* for the 15 mm panel. This correspond to 7200 *N/mm²* and 5133 *N/ mm²* in the E_1 and E_2 direction. For E_3 we have used 200 *N/mm²,* the value is not entirely correct but it will not influence the analysis model more than slightly. It has been difficult to obtain a realistic value for this parameter. For the shear stiffness in the Z-direction $G_1/10$, which is 35 *N/mm²,* is used in approval with Bovim (2011). Transversal shear deformation will be negligible in the thin plywood panels because they are thin, hence Poisson's ratio for plywood is set to 0,1. The metal sheeting is given the default values for S355 in SAP2000.

Table 1 shows the material input data to SAP2000 used in this study.

Table 1: *The material input data used in SAP2000*

Structural-component	**Thickness**	**Material data**
Plywood sheeting	15 mm	Directional symmetry type = Orthotropic Weight per Unit Volume = 4,511e-6N/mm³ (7) Modulus of elasticity E_1= 7 200 E_2= 5 133 N, E_3 = 200 N/mm² (2)(6) Poisson's Ratio, U_1 = 0,1, U_2 = 0,1, U_3 = 0,1 (6) Shear Modulus, G_{12} = G_{13} = 350 N/mm² G_{23} = 35 N/mm² (2)
Metal sheeting	1,2 mm	Weight per Unit Volume = 7,85-05N/mm³ (1)
Support plate	2 mm	Modulus of elasticity, E = 210 000N/mm² (1) Poisson's Ratio, U = 0,3 (4) Shear Modulus G = 81000 (1) Minimum Yield stress, F_y = 355 N/mm²(4) Minimum Tensile Stress, F_u = 400 N/mm²(4)
Wood - C24		Directional symmetry type = Orthotropic Weight per Unit Volume = 4,119e-6 N/mm³ (3) Modulus of elasticity E_1=11 000, E_2 = E_3 = 370 (5)(6) Poisson's Ratio, U_1 = U_2 = U_3 = 0,1 (6) Shear Modulus, G_{12} = G_{13} = G_{23} = 690 N/mm² (6)
GLT - Glued Laminated Timber		Directional symmetry type = Orthotropic Weight per Unit volume = 4,511-6N/mm³ (7) Modulus of elasticity: E_1= 13700, E_2 = E_3 = 420 (5)(6) Poisson's Ratio, U_1 = U_2 = U_3 = 0,1 (6) Shear Modulus, G_{12} = G_{13} = G_{23} = 780 N/mm² (6)
Dummy	15 mm	Same as Metal sheeting/support plate. Section modifiers: weight = 0.

(1) Furulund and Thorrud, 2009
(2) Sintef Byggforsk, Technical approval, Wisa-Spruce plywood
(3) EN338 2009
(4) Default material settings SAP2000
(5) Excel spreadsheet from Lett-Tak AS
(6) Appendix C
(7) Density tests by Furulund and Thorrud.

Appendix C: Fasteners.

In this appendix the different load-displacement curves is handled separately, and commented step by step. The data used to model fasteners is based on Furulund and Thorrud's test, done the spring 2009 which is attached electronic back in this thesis. A 5-parameter Foschi based equation proposed by Girhammar et, al. (2004) are used to fit the curves. The original 3-parameter Foschi equation is extended with two additional parameters, α and β to simulate the point of failure and the softening behavior of the fastener. The Foschi parameters K_0, K_1 and P_0 simulate respectively, slope at initial stiffness, slope at the first asymptote, and interception point on the first asymptote. In figure one to three, load-slip curves from fastener tests (red) and load slip curves from the 5-parameter based Foschi (purple) are shown. In the analyze model, the Foschi based load-slip data is scaled to simulate correct number of fasteners. The load-slip curved used in the analyze models for 600 *mm* lumping of fasteners are shown in figure one to three (blue).

Withdrawal capacity for gable fasteners

Furulund and Thorrud tested the load-carrying withdrawal capacity for lateral loaded 10x100 mm screws to GLT, quality; L40/Gl32c) (2009b). The data used is the averaged of test 1-20, except test 5, 9,10,11,15 and 16 who was clearly deviating from most of the other curves. The excluded curves had softer behavior but with a higher failure load and were taken out to get more realistic data, in agreement with our advisor, Bovim. The failure mode was in all tests embedment failure followed by withdrawal of screws (Furulund and Thorrud, 2009b). Punching of nail head did not occur. The 5-parameter Foschi based data is used only in the link elements in the gable where we expect uplift forces.

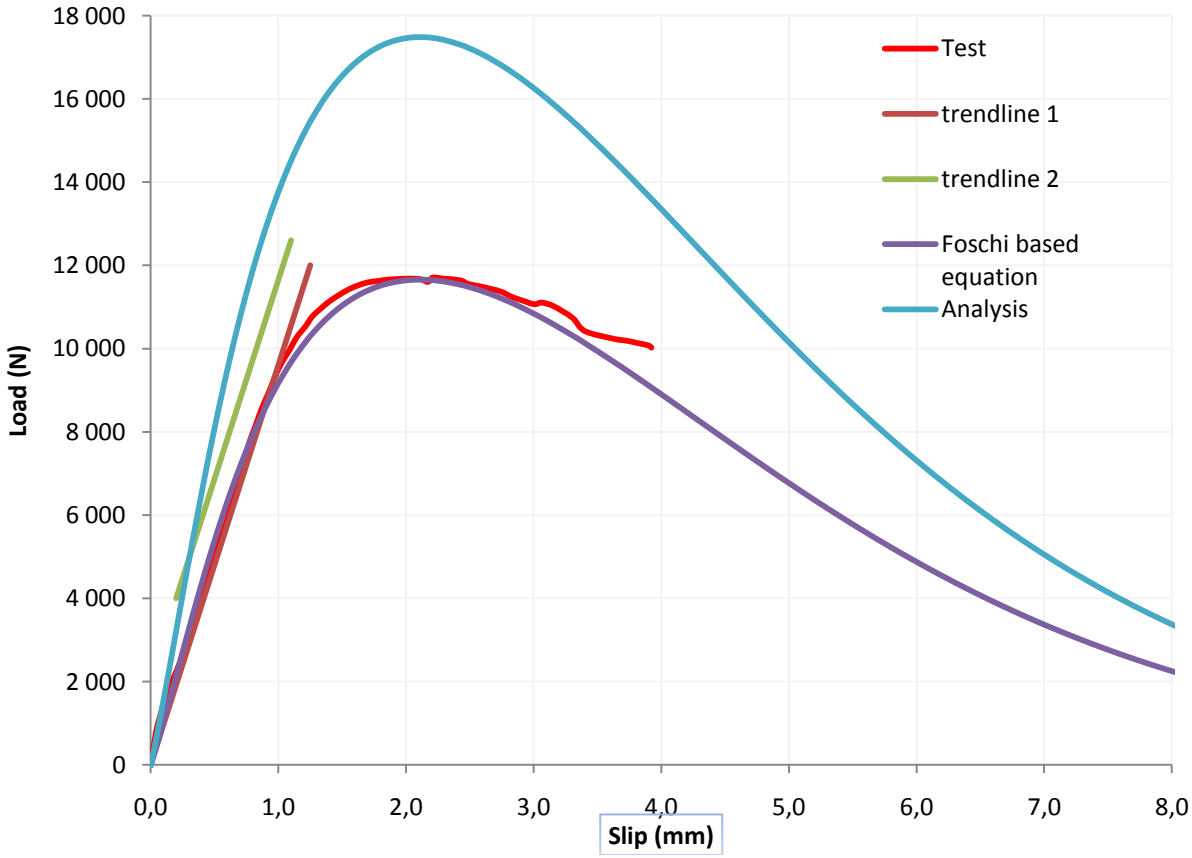

Figure 1; *Load-slip curve gable fasteners withdrawal.*

Shear capacity at gable fasteners

Furulund and Thorrud tested the load carrying shear capacity for a 10x100 *mm* screws for a single shear connection, steel plate (2 *mm* thick) to GLT, quality; L40 /GL32c (Furulund and Thorrud, 2009c). All 20 tests done are included in the average data used by us. The only failure mode that occurred was withdrawal, after two yield hinges in the fastener (Furulund and Thorrud, 2009c) corresponding to failure mode e in Eurocode 5. The 5-parameter Foschi based data is used in the link elements in the metal sheeting to edge-beam joints in the analysis models, respectively in the shear loaded directions.

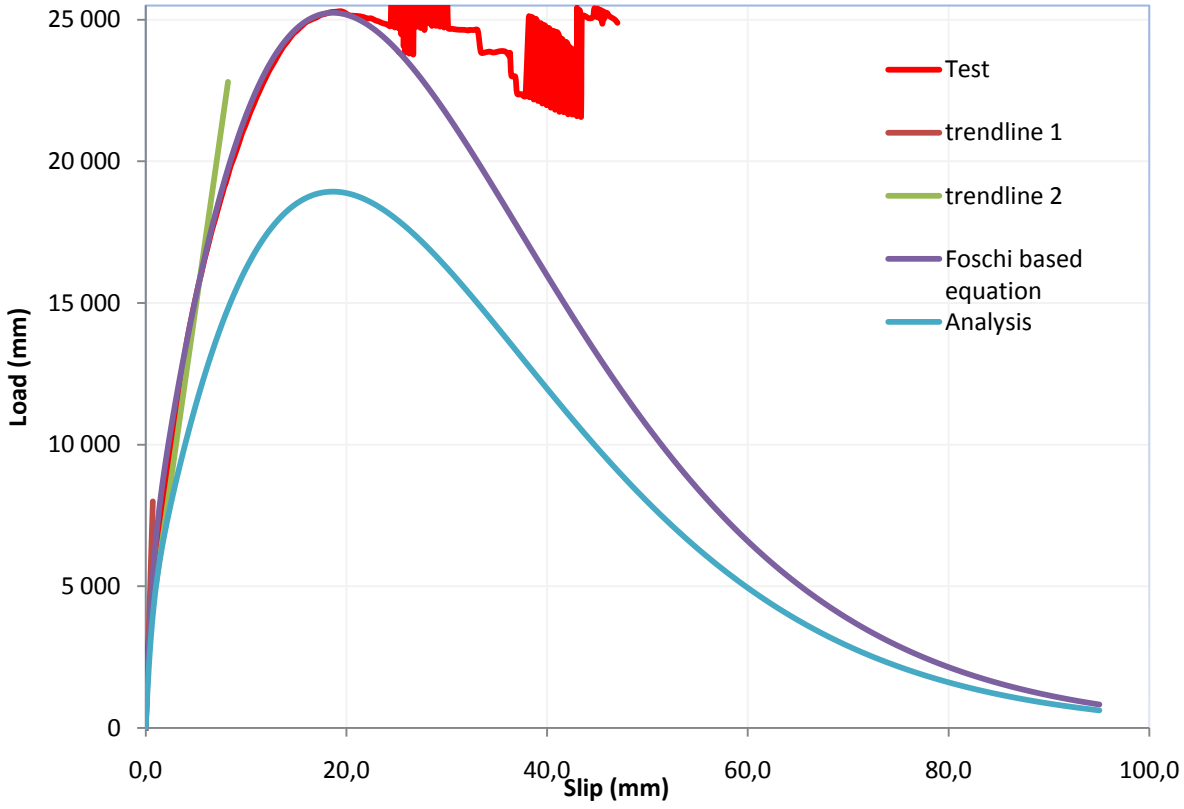

Figure 2; *Load-slip curve gable fastener's shear.*

Shear capacity for fasteners at plywood panel perimeters

Furulund and Thorrud tested the load carrying shear capacity for four 5x45 *mm* screws in a single shear connection, plywood-to-plywood (Furulund and Thorrud, 2009a). The failure mode observed in 19 of 20 tests was embedment failure in both plywood parts followed by withdrawal of the fastener (Furulund and Thorrud, 2009a), which corresponds to failure mode d in Eurocode 5. Punching of nail head occurred in one test. Average of all 20 tests is used. In the load slip curve based on the test data (red curve) we see the initial linear stiffness is followed by a clear bending of the curve at approximately 1,8 *kN* applied load, which is caused by embedment failure in the plywood joint (Bovim, 2011). The next occurrence is stiffening at approximately 3 *kN* applied load. The rope effect may be the best explanation for this stiffening. Data from the 5-parameter Foschi based equation is used for the link elements in the plywood panel butt joint and in the joint connecting plywood to GLT in the analysis model.

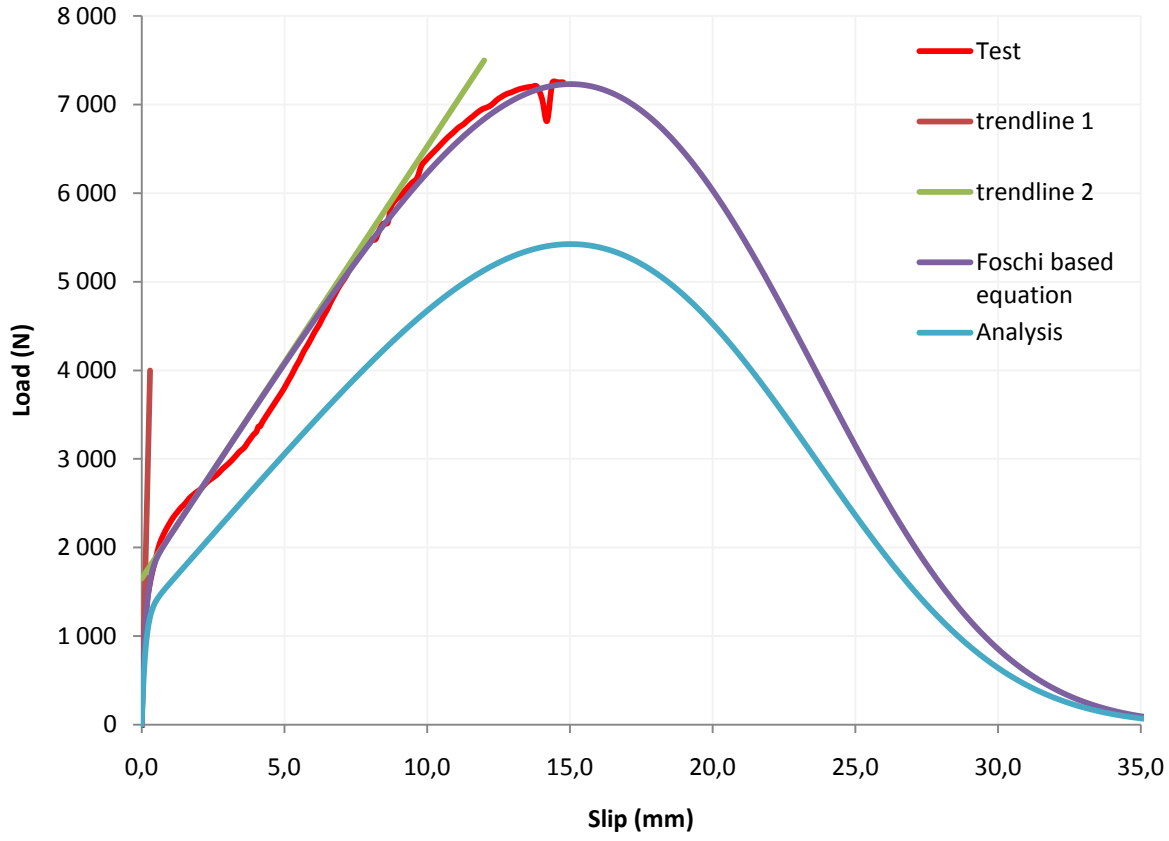

Figure 3; *Load-slip curve plywood perimeter fasteners' shear.*

Withdrawal capacity fasteners at panel perimeters

The experiment done by Furulund and Thorrud (2009d) did not include the withdrawal capacity of the 5x 50 mm fasteners. This means the fasteners at plywood perimeters. The multi-linear lin k element simulating the fasteners needs stiffness in all directions to act realistic. Therefore we have calculated the withdrawal capacity based on Eurocode 5 (CEN, 2004). The calculations are a conservative assumption compared to the real behavior, because the characteristic capacity is based on the lower 5-presentage fractile. The calculations are shown in table 1 and 2. Table 1 shows the characteristic capacity for the fasteners in the plywood panel butt joint, while Table 2 shows the characteristic capacity for the fasteners between plywood and GLT.

Table 1:

Withdrawal capacity fasteners plywood-to-plywood perimeters (CEN, 2004).

$F_{ax,\alpha,Rk}$ =	$n_{ef}*(\pi*d*l_{ef})^{0,8}*f_{ax,\alpha,k}$		
fax,α,k =	$f_{ax,k}/(\sin^2(\alpha)+1,5*\cos^2(\alpha))$		
$f_{ax,k}$ =	$3,6*10^{-3}*\rho_k^{1,5}$		
α =	90,00	°	
n_{ef} =	1,00		
d =	5,00	*mm*	
l_{ef} =	35,00	*mm*	
			(Furulund and Thorrud,
ρ_k=	460,00	kg/m^3	2009d)
$f_{ax,k}$ =	35,52	kg/m^3	
$f_{ax,\alpha,k}$ =	35,52	kg/m^3	
$F_{ax,\alpha,Rk}$ =	5528,27	*N*	

Table 2:

Withdrawal capacity plywood-to-GLT (CEN, 2004).

$F_{ax,\alpha,Rk}$ =	$n_{ef}*(\pi*d*l_{ef})^{0,8}*f_{ax,\alpha,k}$		
fax,α,k =	$f_{ax,k}/(\sin^2(\alpha)+1,5*\cos^2(\alpha))$		
$f_{ax,k}$ =	$3,6*10^{-3}*\rho_k^{1,5}$		
α =	90,00	°	
n_{ef} =	1,00		
d =	5,00	*mm*	
l_{ef} =	45,00	*mm*	
ρ_k=	460,00	kg/m^3	(Furulund and Thorrud, 2009d)
$f_{ax,k}$ =	35,52	kg/m^3	
$f_{ax,\alpha,k}$ =	35,52	kg/m^3	
$F_{ax,\alpha,Rk}$ =	6759,35	*N*	

The values in table 1 and 2 are chosen according to Eurocode 5 (CEN, 2004), the experiments done by Furulund and Thorrud (2009d) and assumptions done with Nils Ivar Bovim (Bovim, 2011).

α : Angle between the grain and the connector, 90 ° .

n_{ef}: number of screws, 1.

d : outer screw diameter, 5 *mm*.

l_{ef} : penetration length. The standard value is the length of the threaded part minus one screw diameter. However we have chosen to set this value to 35 mm for the connection plywood-to-plywood, because the screw is longer than the thickness of the plywood (30 *mm*). Usually the value would be 15 m but beacause this is withdrawal it is natural to assume some sort of friction between the screw and the plywood while it is withdrawn (Bovim, 2011). For the joint between the plywood and the GLT beam we have used the standard value, 50 mm -5 mm = 45 *mm*.

ρ_k : The density of the wood, determined in the experiment by Furulund and Thorrud, 460 kg/m^3 for both the plywood and the GLT.

As shown in table 1 and 2 the withdrawal capacity of the screws is 5528 B and 6759 N for respectively the plywood-plywood seam and the plywood-GLT seam. In the force deformation curves used in SAP2000 we have assumed the screws to reach it's maximum capacity when it is withdrawn one thread length. One thread length is 2 *mm*, the force-deformation curves are shown in figure 1 and 2 (Bovim, 2011). The link distance for the data shown is 600 *mm*.

Figure 1:
Force-deformation curve plywood-plywood seam. Link distance = 600 mm

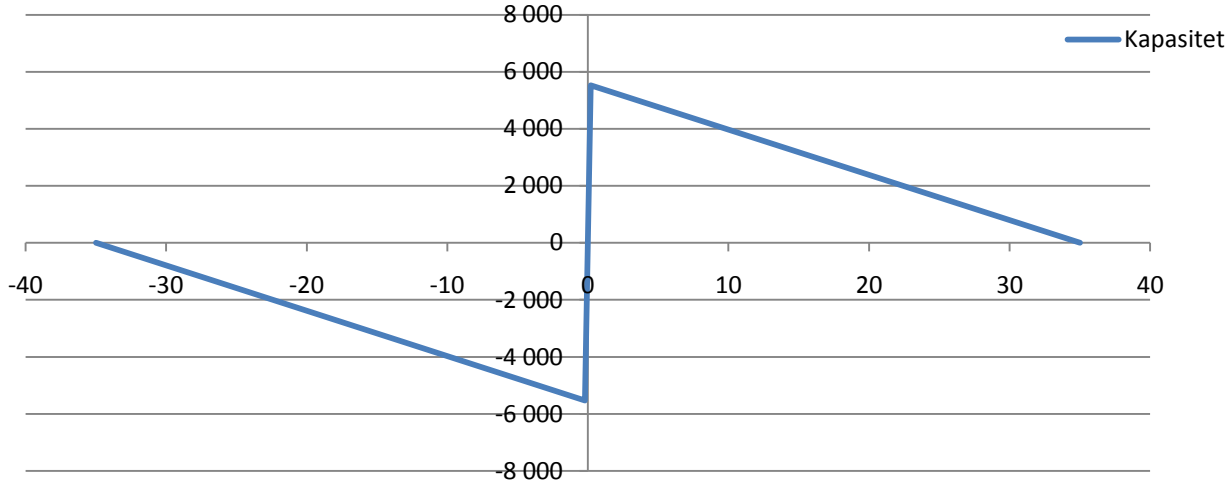

Figure 2: *Force-deformation curve plywood-GLT. Link distance = 600 mm*

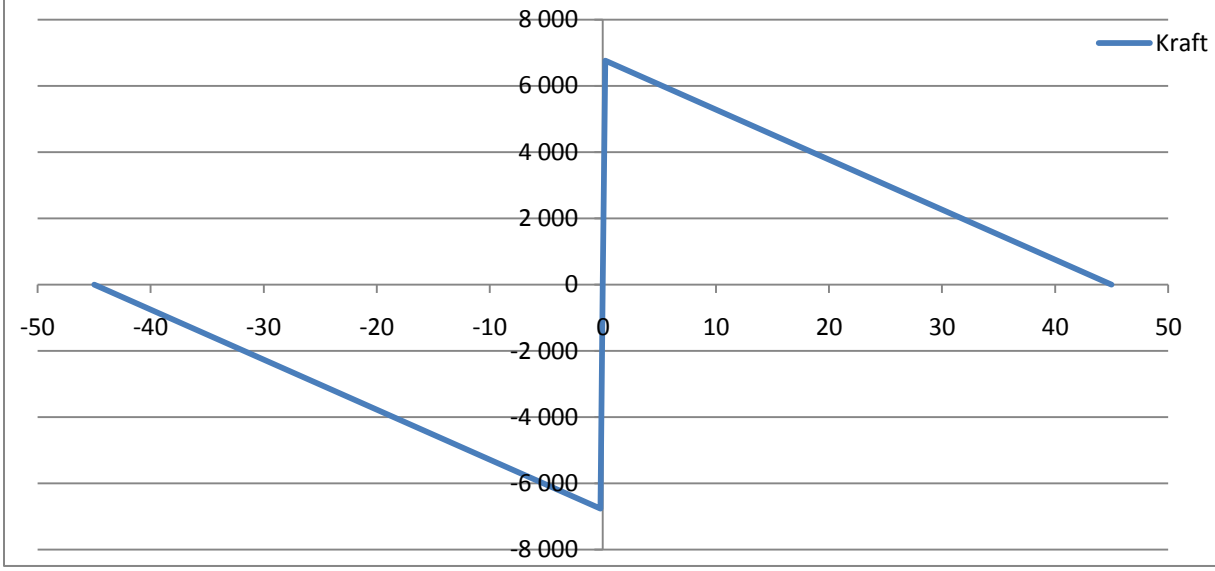

APPENDIX D: The torsion stiffness of the elements.

This appendix is a comparison of the modeled and the theoretical torsion stiffness from Rindal (2009).Eli Bjørhovde Rindal calculated the light weight roof element's rotation stiffness, and tested it versus a FE-model made in Focus 2D. To test the rotation stiffness of our models we have taken sections from both models. The sections have been assigned with the same restraints as the light weight roof elements in Rindal's thesis. The torsion moment calculated in Rindal rotates the light weight roof element 1° . Rindal's calculations were done on light weight roof elements with a metal sheeting height of 360 *mm* while our models have a height of 310 *mm*. Hence we had to do some adjustments to be able to compare the models. The material data used in our calculations are shown in table 1. The calculation of the torsion stiffness of the 310 *mm* light weight roof element is shown below. The formulas are the same as Rindal used. The setup of the models is shown in figure 1 and figure 2.

Torsion stiffness D:

The equations are taken from Rindal (2009).

$$D = G * J$$

$$J = 4 * \frac{b_{steel} * (\left(h_{steel} + h_{wood} + \frac{t_{ply}}{2}\right))^2}{\frac{h_{steel} * 2 + b_{bottom,\ steel}}{t_{steel}} + \frac{b_{ply} * G_{steel}}{G_{ply} * t_{ply}}}$$

$$\text{J}= \left(4* \frac{310* \left(\left(310+71+\frac{15}{2}\right)\right) 2}{\frac{310*2+500}{1,2}+\frac{600*80000}{360*15}} \right) = 16\ 302\ 754\ mm^4$$

Torsion moment M_T:

$$M_T = \frac{\pi * G * J}{180 * L_{element}}$$

$$M_T = \left(\frac{\pi * 80000 * 16302754}{180 * 10000}\right) = 2276283\ N\ mm$$

Table 2 shows the rotations due to the moment in the neutral axis of the element. There are some differences in the rotation, both models have more rotation than Rindal's element. The reason for the difference between Rindal's model and the shell model may be the assumptions done by Rindal and the difference in detailing of the two models. The beam model doesn't seem to have sufficient rotation stiffness, due to the nature of the non-prismatic beam element. It seems like the beam sections should have been modeled as a closed section to have the correct torsion stiffness.

Table 1: *Material data for calculation of the rotation stiffness.*

Sheeting metal:			**Wood row:**			**Plywood panel**		
h_{steel} =	310	*mm*	H_{wood} =	71	*mm*	t_{ply} =	15	*mm*
b_{steel} =	515	*mm*				b_{ply} =	600	*mm*
$b_{bottom,steel}$ =	500	*mm*				G_{ply} =	360	N/mm^2
t_{steel} =	1,2	*mm*						
G_{steel} =	80000	N/mm^2						

Table 2: *Rotations in the element due to the moment.*

Model:	**Moment (*Nmm*)**	**Rotasjon(°)**
Theoretical	2 748 534	1
Focus 2D	2 748 534	1,0004
Shell model	2 276 283	1,55
Beam model	2 276 283	6,87

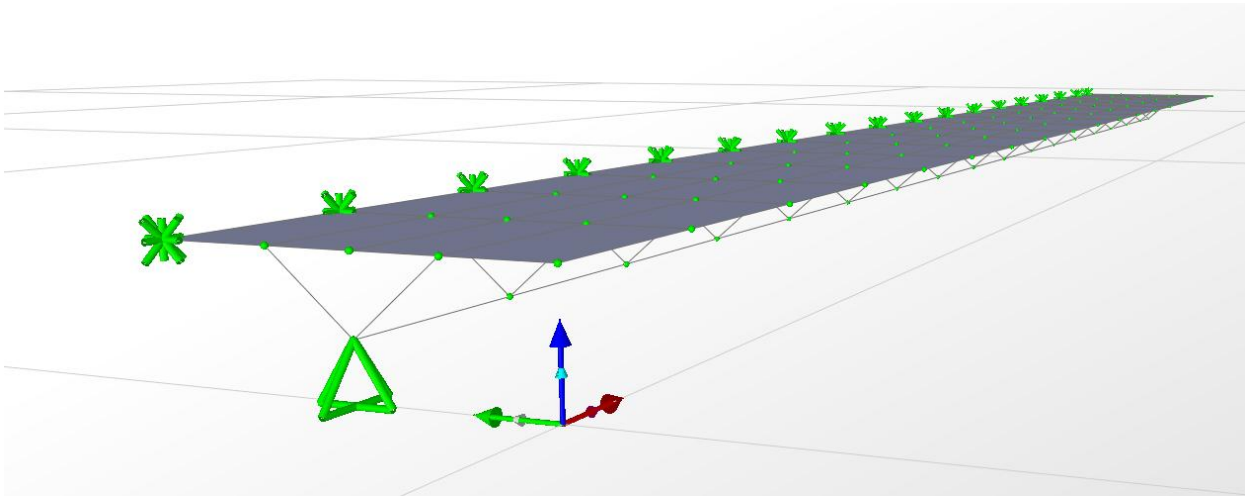

Figure 1: *Beam model in 3D from SAP2000.*

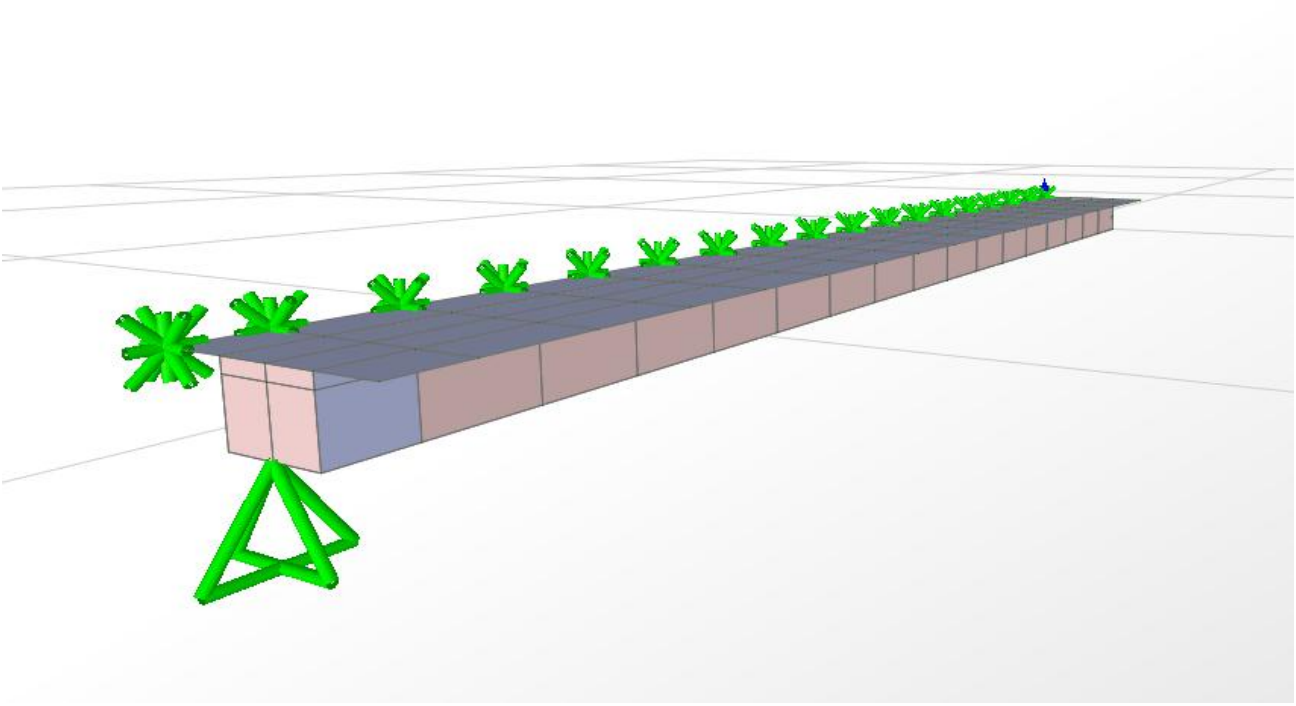

Figure 2: *Shell model in 3D from SAP2000.*

Appendix E: Analysis method

This appendix is a supplement to chapter 2.4.4 in our thesis. To explain more about the analysis method and values used in the study.

There are a wide variety of analysis methods in SAP2000, static, nonlinear, modal, non-linear pushover analysis etc. (CSI, 2010b). To model the nonlinear effect of the model, the p-delta effects and the non-linear behavior of the connectors we had to use nonlinear static analysis. Typical nonlinear behavior is local buckling, uplift at foundation, contact between members and yielding (Wilson, 2004). There are several types of nonlinearity in SAP2000: Material nonlinearity, geometric nonlinearity and staged construction (CSI, 2010b). SAP2000 uses the fast nonlinear analysis (FNA) method to analyze nonlinear behavior. FNA is faster and more accurate compared to the traditional analysis methods for nonlinear analysis (Wilson, 2004). The traditional methods for analysis is using exact eigenvectors to solve their problems, FNA uses load dependent Ritz vectors for accurate results and less computational time (Wilson, 2004).

The P-delta effects are displacements due to for example lateral movements in a building giving it second-order moment. The geometric stiffness matrix of the structure or element is used to take the P-delta effects into account in SAP2000 (Wilson, 2004, Schueller, 2008). There is an option to choose between P-delta analysis and P-delta analysis with large deformations (CSI, 2010b).

For the P-delta analysis the equilibrium equations take the deformed shape into partial account. Geometric nonlinearity makes SAP2000 do iterative steps when modeling P-delta effects. P-delta plus large deformations are for structures where the geometric nonlinearity dominates, examples are structures with cables or for buckling analyses. A P-delta analysis is usually adequate if none of the elements above are present, particularly when material linearity dominates. We have chosen to use P-delta analysis.

In the nonlinear static analysis there are several options in addition to the P-delta analysis, to get an accurate analysis you have to have the parameters correctly. The correct values have to be chosen by testing different setups until you get consistent results. The total amount of steps, total null steps, iterative steps per step, relative unbalance and relative convergence tolerance are all important parameters (CSI, 2010b). The relative convergence tolerance is set to 0, 0001 as

default, the relative unbalance is influenced by the relative convergence tolerance and the convergence tolerance. The convergence tolerance is found by multiplying the relative convergence tolerance and the current magnitude of the load vector(CSI, 2010b). The system reaches its solution when the relative unbalance is less or equal to 1,0(CSI, 2010b).

A null step is when: a frame hinge trying to unload, an event triggers another event or iteration does not converge and a smaller step size is attempted (CSI, 2010b). A large number of null steps may indicate that the model is unstable or has elements which are not connected.

To make sure that equilibrium is reached for every step SAP2000 uses iterations. For each step there are a certain number of iterations, first constant-stiffness iterations (Default = 10 iterations). If necessary SAP2000 uses Newton-Raphson iterations (default= 40 iterations) in addition to the constant-stiffness iterations. If both of the iterations fail the step size is reduced and the procedure is done again.

For our analysis we started with the default values, and tested the models. In the early stages the model was unstable and we had to use a large amount of null steps, total steps and relative convergence tolerance to get the analysis to converge. This was especially the case for the load cases with large forces, because of the large deformations. When the model developed into the final model we tried different values for the input data, and found that the values giving the best results were the default values.